4

Results from a field in the constellation Lyra

My God - it's full of stars!
David Bowman, in "2010: Odyssey Two"

In this chapter, we make a detailed presentation of the results of a TrES campaign pointed towards a field in the constellation of Lyra. A total of 16 transiting planet candidates were identified, and follow-up observations together with a detailed analysis of the light curves were performed to identify the false positives. We describe the results for each of the candidates, which finally allowed the identification of 15 false positives, and a transiting planet, TrES-1, which will be discussed in the next chapter.

4.1 Observations

THE field of Lyra was centered on the star Theta Lyrae (RA $=19^h16^m22.10^s$ $\delta = +38°08'01.4''$, J2000.0, V= 4.347, b=11.86°), and observed for 49 good nights (July 1st until September 16th), from the STARE site (Tenerife, Spain), and 25 good nights from the PSST site (Lowell, Arizona, USA). The Sleuth telescope was still under development at that time, and so did not observe this field. For about another 7 nights the STARE's guiding system didn't work properly, and these images were not further analyzed. PSST had also some technical problems for ∼43 days during their observing season, and thus only the 25 nights mentioned above were useful.

Bias series of 20 images were taken at the beginning of each night, and

later on averaged to have one master bias for every night. Dome and twilight flats were obtained approximately at the middle of the observing season, and a combination of these flats was performed as described in Chapter 2. Only one master flat field image was used to correct all the 10166 (final 8868) science images. Some experiments using more than one master flat field image for the reduction of a whole campaign resulted in significant (several percent) jumps in the final light curves, which arose from an incomplete correction of the different pixel sensitivities. This can be due to slight variations in the position of the telescope + dome while taking the dome flats, or to poor statistical significance of the master flat images (taken as an filtered average of 20 images in the case of dome flats and typically 8 images in the case of the sky flat images). Even with the risk of not achieving a correct absolute calibration (which would in any case need to be handled with care, as we saw in Chapter 2), we preferred to have the same flat field correction for every image, as we are interested in differential changes.

4.2 Data reduction

Data were processed as described in Chapter 2. Here we outline some details of interest.

When running DAOPHOT/PHOT (Stetson 1992) on the image used to obtain the standard star list, we got 56000 stars with a signal greater than 10 sigmas above the sky background. As we do not expect to have enough precision in the faintest stars to find planetary transits, we set a threshold of 25 sigma for the signal, resulting in ∼31000 stars in the final star list.

The master image for the field was built from an average of 17 images taken around the same time as the image used to build the star list. It is plotted in figure 4.1.

The standard deviation of the stars achieved for this field, for the 9-min binned STARE data, goes down to 3 mmag in the bright end, and rises above 10 mmag after 5700 stars. A plot of the rms of the stars versus magnitude is given in figure 4.2. The bright end of the plot shows some dispersion which can be due to saturation effects: the reference image used to build the standard starlist was chosen in a clear moonless night, with the lowest sky-background level. The brightest stars, in a night with a higher sky background level, will be closer to the saturation value, or even saturated.

As a comparison, we plot in Figure 4.3 the rms for the PSST observing run. This data set is shorter, and it becomes clear from this plot the advantage of having a back-illuminated CCD instead of a front-illuminated one such as STARE's (for details, see the Table 2.1 in the Chapter 2): the detector is

sensitive to fainter stars, and the final dispersion in the light curves is smaller. We are planning to upgrade the STARE detector in the present year.

4.3 Transit candidates

We performed a search for transiting planet candidates with the BLS algorithm (Kovács, Zucher, & Mazeh 2002) on the brightest 12000 stars, divided in blocks of 2000 stars. The threshold was chosen by visual inspection of the final SDE (Spectral Distribution of Energy, see Equation 2.13) of the 2000 stars; typically, fixing the threshold where the approximately gaussian-shaped signal has $\sim 1/3$ of its maximum value, returns a number of false positives that are easily recognized by visual inspection of the light curves. This threshold was established as SDE=2.7 Examples of such false positives are plotted in Figure 4.4.

After the visual inspection of all the stars returning values above the threshold, and discarding the obvious outliers (eclipsing binaries, variable stars, stars too close to the edges of the CCD or to dirty parts, not fully corrected with the flat field images), we ended up with a list of 16 transiting planet candidates. Ordered in increasing period, they are plotted in Figures 4.5 and 4.6, and summarized in Tables 4.1, 4.2 and 4.3. After this first identification of the candidates, we refined the period determination, by running the BLS algorithm with a better phasing coverage and oversampling: The frequencies in region with a width of 0.1 c/d around the corresponding peak[1] were sampled, and a conservative period error estimate was computed as the difference between the values of the period in which the SDE peak amplitude decreased to half of its maximum level. The folded light curves in Figures 4.5 and 4.6 were constructed using this refined period estimation. We have kept the original values of the SDE (i.e., those obtained after the first BLS pass), even if the periods were not exact, to reflect the significance of each detection.

[1] In several of the candidates, we found that the highest amplitude peak was not the real period of the candidate, but an integer multiple of its period. Visual inspection of the folded light curves helps to identify the correct peaks. This was the case of T-Lyr0-03507, as we will see in the Section 4.5.9

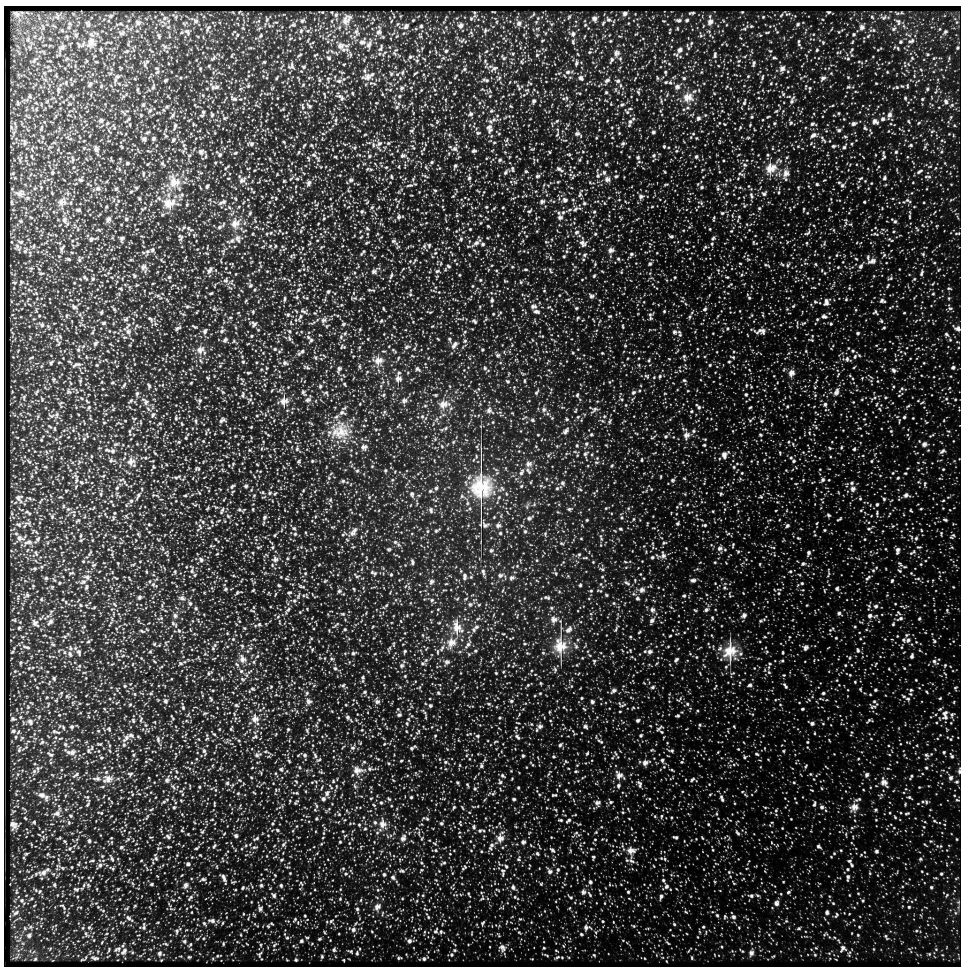

FIGURE 4.1— Master image of a field centered in the constellation Lyra.

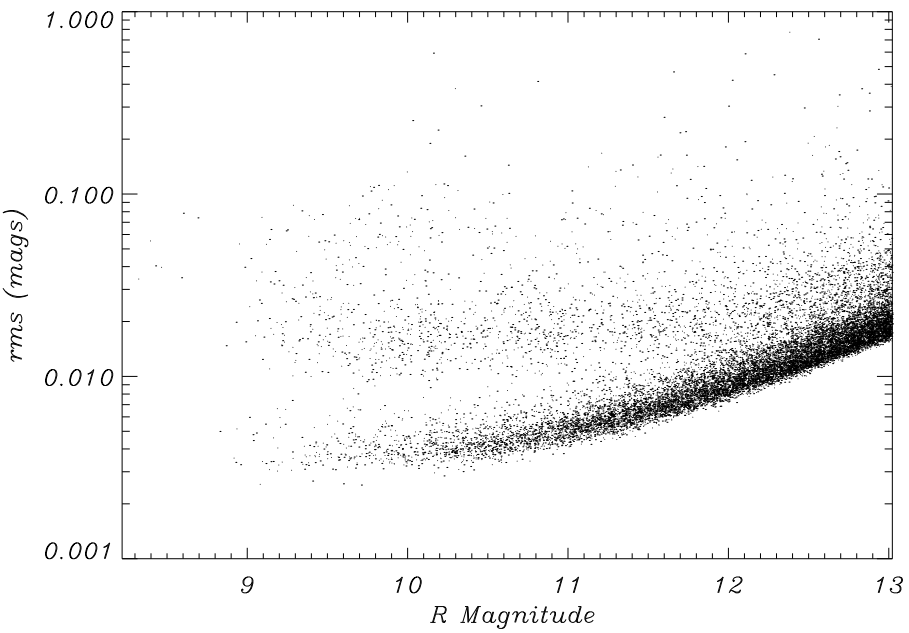

FIGURE 4.2— The rms versus magnitude for the Lyra run. Each point represents the rms of a star in the 9-min binned data, for the whole run. STARE data.

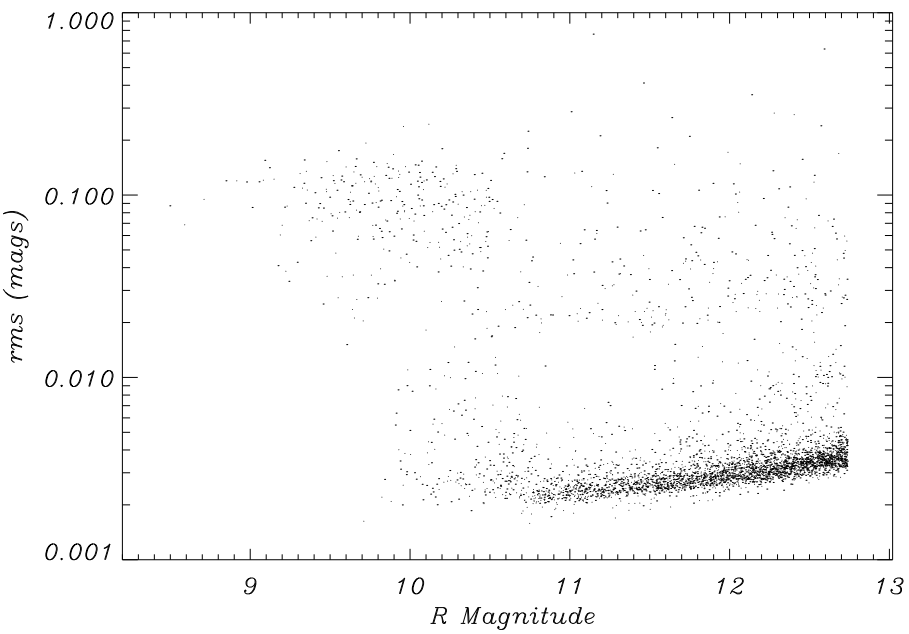

FIGURE 4.3— Same as Figure 4.2, but for the shorter PSST data set.

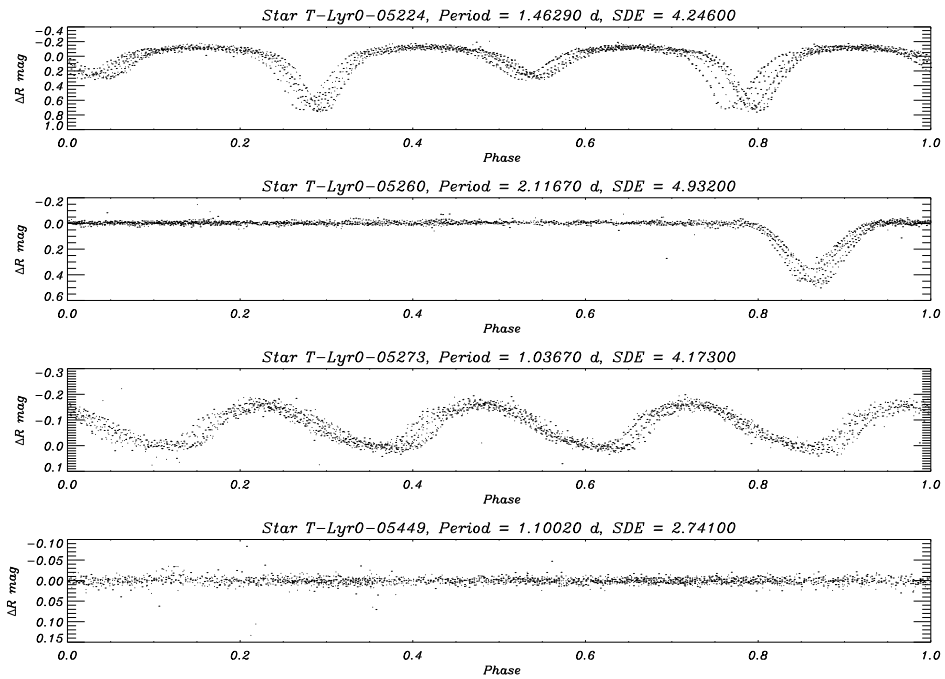

FIGURE 4.4— False positives from the BLS search, easily recognizable by visual inspection. From top to bottom: Two eclipsing binaries, one pulsating star and a star with a SDE close to the threshold of detection, not showing any evidence for a transit-shaped feature.

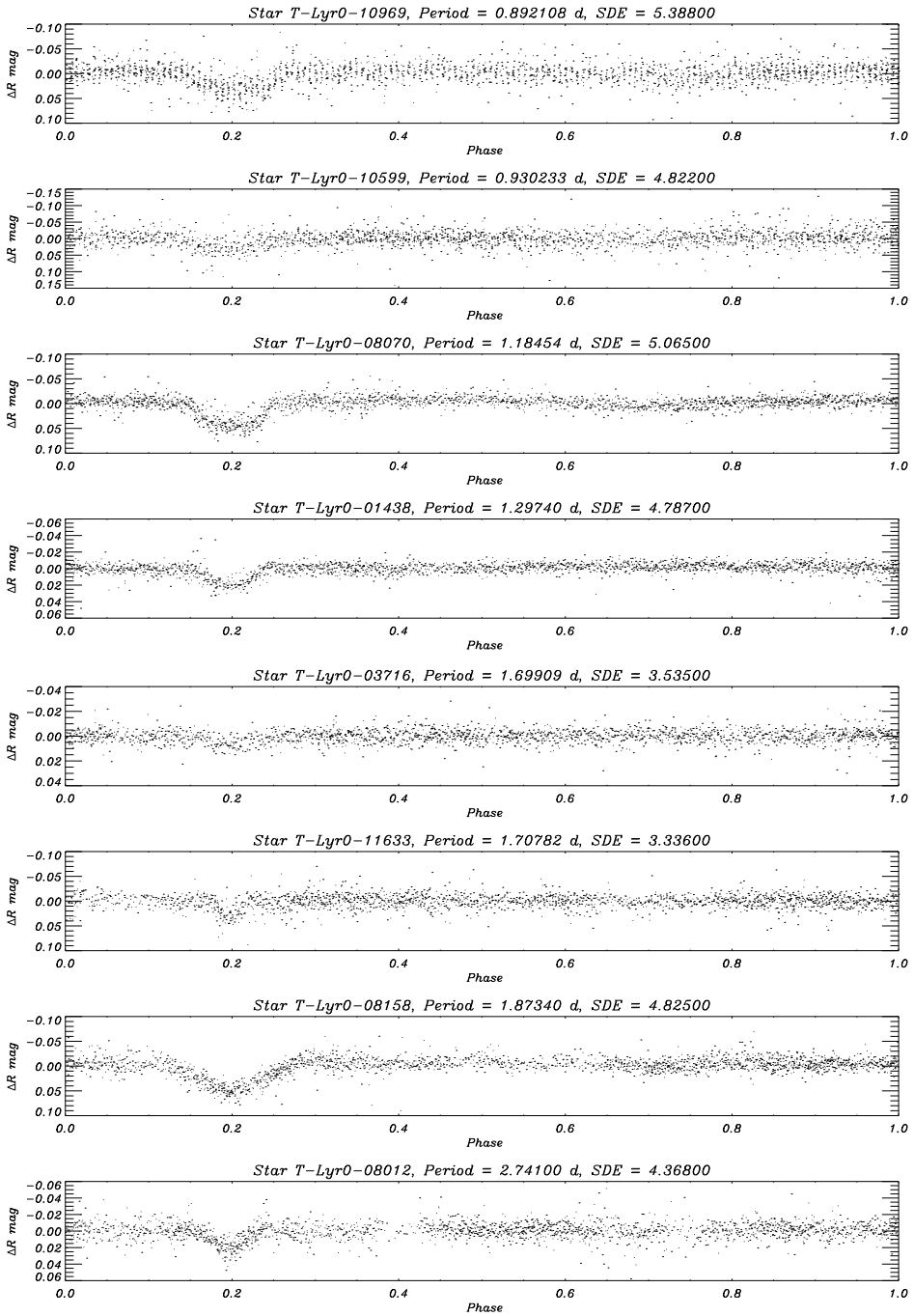

FIGURE 4.5— Folded light curves of transit candidates in the Lyra field.

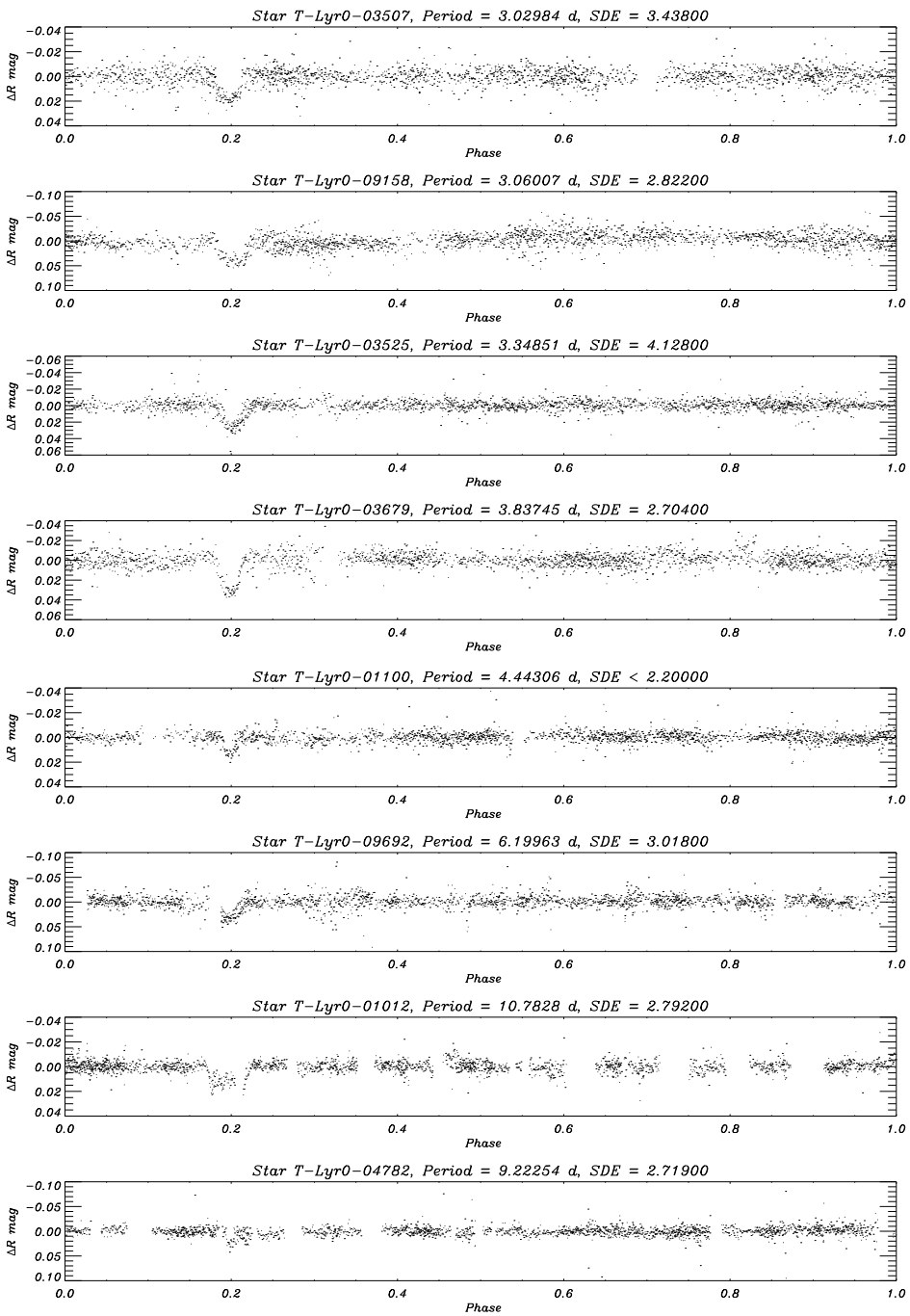

FIGURE 4.6— Folded light curves of transit candidates in the Lyra field.

TABLE 4.1— Characteristics of the stars showing transit-like events.

Candidate ID	GSC 1.2 ID	2MASS coordinates	2MASS J	2MASS H	2MASS K	USNO ppm ra (err)	USNO ppm dec (err)	Sp. Type (J-H)	Sp. Type (H-K)
T-Lyr0-10969	02666-01877	19 27 56.3 +36 13 19	11.857	11.667	11.638	0(0)	0(0)	F3	F0
T-Lyr0-10599	NO	19 29 47.7 +35 58 12	11.759	11.536	11.497	0(0)	0(0)	F5	F5
T-Lyr0-08070	03121-01659	19 19 03.6 +38 40 56	11.507	11.321	11.261	0(0)	8(0)	F3	G6
T-Lyr0-01438	02665-01287	19 17 08.6 +36 24 57	9.761	9.520	9.489	2(0)	8(0)	F6	F1
T-Lyr0-03716	02655-01344	19 16 41.1 +36 55 35	10.103	9.588	9.435	0(0)	0(0)	K2	K8
T-Lyr0-11633	02655-01623	19 14 58.7 +36 48 44	11.816	11.569	11.518	4(2)	-6(1)	F6	G1
T-Lyr0-08158	03134-00705	19 21 54.5 +38 25 37	10.935	10.375	10.253	0(0)	0(0)	K3	K6
T-Lyr0-08012	03121-00781	19 17 52.3 +38 52 02	11.162	10.907	10.820	-6(5)	10(1)	F6	K2
T-Lyr0-03507	02652-01324	19 04 09.8 +36 37 57	10.294	9.887	9.819	-42(0)	-22(0)	G8	G8
T-Lyr0-09158	02652-01397	19 11 39.? +36 49 03	11.201	10.829	10.780	8(2)	8(2)	G6	G0
T-Lyr0-03525	03125-00317	19 13 05.? +40 24 02	10.587	10.415	10.362	-4(0)	20(0)	F3	G3
T-Lyr0-03679	02665-00795	19 20 33.9 +36 37 32	10.362	9.870	9.748	0(0)	0(0)	K1	K6
			12.159	11.765	11.649			G8	K5
T-Lyr0-01100	03125-01126	19 13 53.3 +40 05 16	10.364	10.134	10.093	0(0)	0(0)	F5	F5
		19 13 53.8 +40 05 08	10.764	10.555	10.515			F4	F5
T-Lyr0-09692	03120-00359	19 04 37.1 +39 03 56	11.408	11.160	11.057	-4(5)	-14(0)	F6	K4
T-Lyr0-01012	02666-00345	19 28 09.1 +36 44 45	9.723	9.611	9.564	0(0)	-8(0)	A8	F8
T-Lyr0-04782	03124-02558	19 01 10.7 +39 56 49	9.664	8.821	8.621	-2(1)	-6(2)	M?	M1

TABLE 4.2— Characteristics of the transit-like events (I).

Candidate ID	Period (d)	Epoch (HJD-2450000.)	Duration (h)	Depth (mags)	Fainter close stars[1] Distance and ΔJ	Flat Bottom Duration (h)
T-Lyr0-10969	0.892108	2821.94014	2.45	0.031	20″,2.45 mags	1.53
T-Lyr0-10599	0.930233	2821.45589	3.13	0.026	27″,2.87 mags, 33″,1.47 mags	1.33
T-Lyr0-08070	1.184539	2824.46888	2.89	0.040	37″,0.81 mags	1.78
T-Lyr0-01438	1.297404	2821.22555	2.73	0.019	13″,2.61 mags	1.03
T-Lyr0-03716	1.699091	2822.32172	4.81	0.007	7.9″,2.87 mags	0.46
T-Lyr0-11633	1.707825	2822.33848	1.95	0.030	11″,2.00 mags, 14″,2.79 mags	0.52
T-Lyr0-08158	1.873396	2821.59657	6.64	0.052	9″,2.44 mags	0.38
T-Lyr0-08012	2.741003	2822.76567	4.50	0.025	21″,2.04 mags	-0.13(0)
T-Lyr0-03507	3.029844[a]	2820.16941	2.51	0.018	NO	1.64
T-Lyr0-09158	3.060069	2821.02118	3.25	0.040	34″,0.46 mags	1.69
T-Lyr0-03525	3.348513	2820.68971	3.56	0.026	22″,2.91 mags	0.51
T-Lyr0-03679	3.837446[a]	2821.01704	2.97	0.031	7.8″,1.80 mags	1.28
T-Lyr0-01100	4.443060	2820.86708	2.43	0.014	8″,0.40 mags	0.45
T-Lyr0-09692	6.199628	2821.23664	6.99	0.033	NO	1.37
T-Lyr0-01012	10.782834	2825.48893	13.46	0.013	NO	10.46
T-Lyr0-04782	9.222540	2834.49387[b]	?	0.028	NO	?

[1] At an apparent distance lower than 40″ and with ΔJ lower than 3 mags

[a] These epochs and periods are refined later on this thesis, with further observations.

[b] Epoch of the single observed eclipse.

TABLE 4.3— Characteristics of the transit-like events (II).

Candidate ID	Period	N	events		Follow-up work resuts
	(d)	W	I	E	
T-Lyr0-10969	0.892108	5	6	3	Blended system, eclipsing F+brown dwarf system, or F+M system
T-Lyr0-10599	0.930233	3	3	2	Triple blended system
T-Lyr0-08070	1.184539	7	5	4	Binary system (F+M)
T-Lyr0-01438	1.297404	5	5	2	Binary system, double the period (similar components)
T-Lyr0-03716	1.699091	3	1	1	Triple blended system
T-Lyr0-11633	1.707825	5	0	2	Binary system
T-Lyr0-08158	1.873396	3	5	4	Blended system, double the period[b]
T-Lyr0-08012	2.741003	3	2	3	Blended system?[b]
T-Lyr0-03507	3.029844[a]	3	1	0	Transiting planet
T-Lyr0-09158	3.060069	2	0	1	Binary system
T-Lyr0-03525	3.348513	3	0	2	Binary system
T-Lyr0-03679	3.837446[a]	1	1	2	Blended system[b]
T-Lyr0-01100	4.443060	2	0	1	Blended system[b,c]
T-Lyr0-09692	6.199628	0	0	3	Triple blended system?
T-Lyr0-01012	10.782834	1	1	1	Binary system
T-Lyr0-04782	9.222540	1	0	0	Unsolved case

[a] These epochs and periods are refined later on this thesis, with further observations.

[b] Resolved in the 2MASS images.

[c] Resolved with AO observations (NAOMI at 4.2 m WHT).

TABLE 4.4— Stellar densities from *i*) values tabulated at Cox (2000), where the spectral types of the stars are estimated from the 2MASS J–K colors (Bessell & Brett 1988), and *ii*) the result of fitting the transit shape, as proposed by Seager & Mallén-Ornelas (2003). Main sequence stars and circular orbits for the companions have been assumed.

Candidate ID	J–K	Sp. Type (J–K)[1]	$\log(\rho/\rho_\odot)_{(J-K)}$	$\log(\rho/\rho_\odot)_{(Fit)}$	$\Delta = \log(\rho/\rho_\odot)_{(J-K)} - \log(\rho/\rho_\odot)_{(Fit)}$	10^{Δ}
T-Lyr0-10969	0.219	F5	-0.20	-0.46	0.26	1.82
T-Lyr0-10599	0.262	F5	-0.14	-0.63	0.49	3.09
T-Lyr0-08070	0.246	F5	-0.16	-0.35	0.19	1.55
T-Lyr0-01438	0.272	F5	-0.12	-0.66	0.54	3.47
T-Lyr0-03716	0.668	K5	0.15	-1.57	1.72	52.5
T-Lyr0-11633	0.298	F5	-0.09	-0.79	0.70	5.01
T-Lyr0-08158	0.682	K5	0.17	-1.37	1.54	34.7
T-Lyr0-08012	0.342	G0	-0.04	-0.99	0.95	8.91
T-Lyr0-03507	0.475	K0	0.05	-0.02	0.07	1.17
T-Lyr0-09158	0.421	G5	0.02	-0.23	0.25	1.78
T-Lyr0-03525	0.225	F5	-0.19	-0.66	0.47	2.95
T-Lyr0-03679	0.614	K0	0.11	-0.14	0.25	1.78
T-Lyr0-01100	0.249	F5	-0.16	-0.14	-0.02	0.95
T-Lyr0-09692	0.351	G0	-0.04	-0.99	0.95	8.91
T-Lyr0-01012	0.159	F0	-0.31	-1.48	1.17	14.8
T-Lyr0-04782						

[1] Spectral type of the star with the closest J–K color in the Bessell & Brett (1988) tables.

[2] From a 4^{th} order polynomial fit to the J–K vs $\log(\rho/\rho_\odot)$ in the tables of Cox (2000)

4.4 Careful inspection of the transit candidates

As we saw in the previous Chapter, a careful interpretation of the light curves of the candidates can reveal false positives, without the need for further telescope time. In this Section, we apply two different tests to the candidates obtained in the Lyra field, based on the transit shape and on the out of eclipse modulation.

4.4.1 Stellar densities

To show the utility of a detailed light curve analysis, we applied the formulation described in Chapter 3, in Section 3.2.2, which allows a measurement of the host star density. This can be compared with the density inferred from the 2MASS colors, according to the values tabulated in Cox (2000). As there are few tabulated values in these tables, we performed a 4^{th} order polynomial fit of the J–K vs $\log(\rho/\rho_{\odot})$, and used the fitting coefficients to estimate the $\log(\rho/\rho_{\odot})$ of each candidate from its J–K color.

Fits of the transit shapes with the function defined in Section 3.2.2 are plotted in Figures 4.7 and 4.8. To provide a cleaner view of the transit shape, Figures 4.9 and 4.10 plot the phases of transit for each of the candidates, with the data points binned in 0.005 wide phase-bins. The error bars are the rms of the N points inside each bin, divided by the square root of N.

The results are summarized in Table 4.4, where the last column shows the ratio among the stellar densities estimated from the J–K 2MASS colors and those resulting from the transit shape fitting. There are only 3 stars for which this factor is in the range [0.4-1.6], which means that the two measurements of the densities differ by less than 60%.

This method eliminates 13 of the 16 candidates. These are T-Lyr0-08070, T-Lyr0-03507 and T-Lyr0-01100. For long-period candidates (in the frame of ground based transit searches, i.e., periods bigger than $\sim$7 d), this test should not be considered as a final test, as the eccentricities of the known exoplanets with these periods begin to become significant (e.g., HD 217107b, with a period of 7.11 d and an eccentricity of 0.14, Fischer et al. 1998), and the test intrinsically assumes circular planetary orbits. Of particular significance are the candidates whose J–K colors are typical of a K star; some of them have ratios among the two densities of several tens, which provides a clue that the K star is not a main sequence star (as assumed in the test) but a red giant. This is a strong indication for a blended system, as the typical radii of the giants (several tens of the solar radius) does not allow orbits with the short periods usually found by the observations (the orbit would be inside the stellar atmosphere).

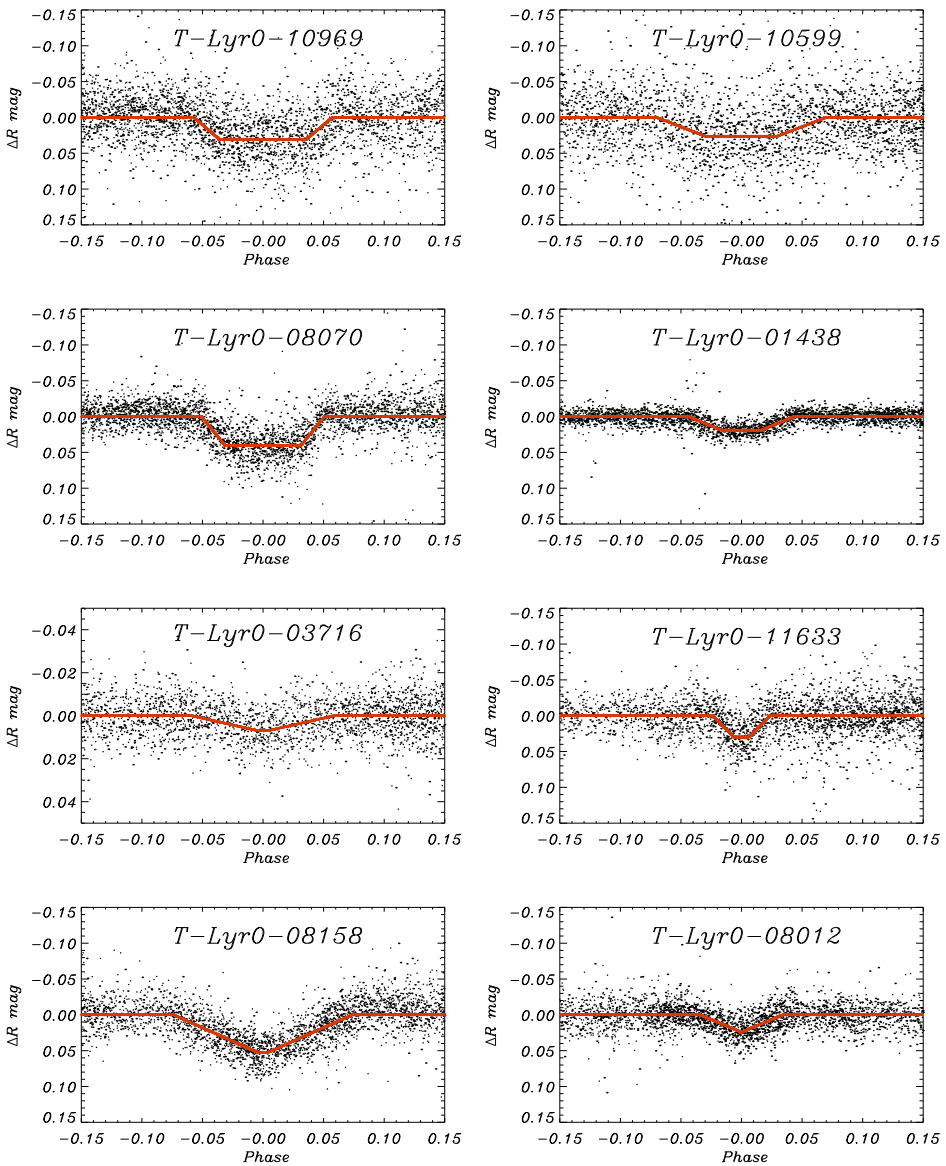

FIGURE 4.7— Transit shape fitting of the candidates in the Lyra field. The free parameters in the least square fit were the phase of the center of the transit, its total duration, depth and ingress (equal to the egress) time. See the text for details.

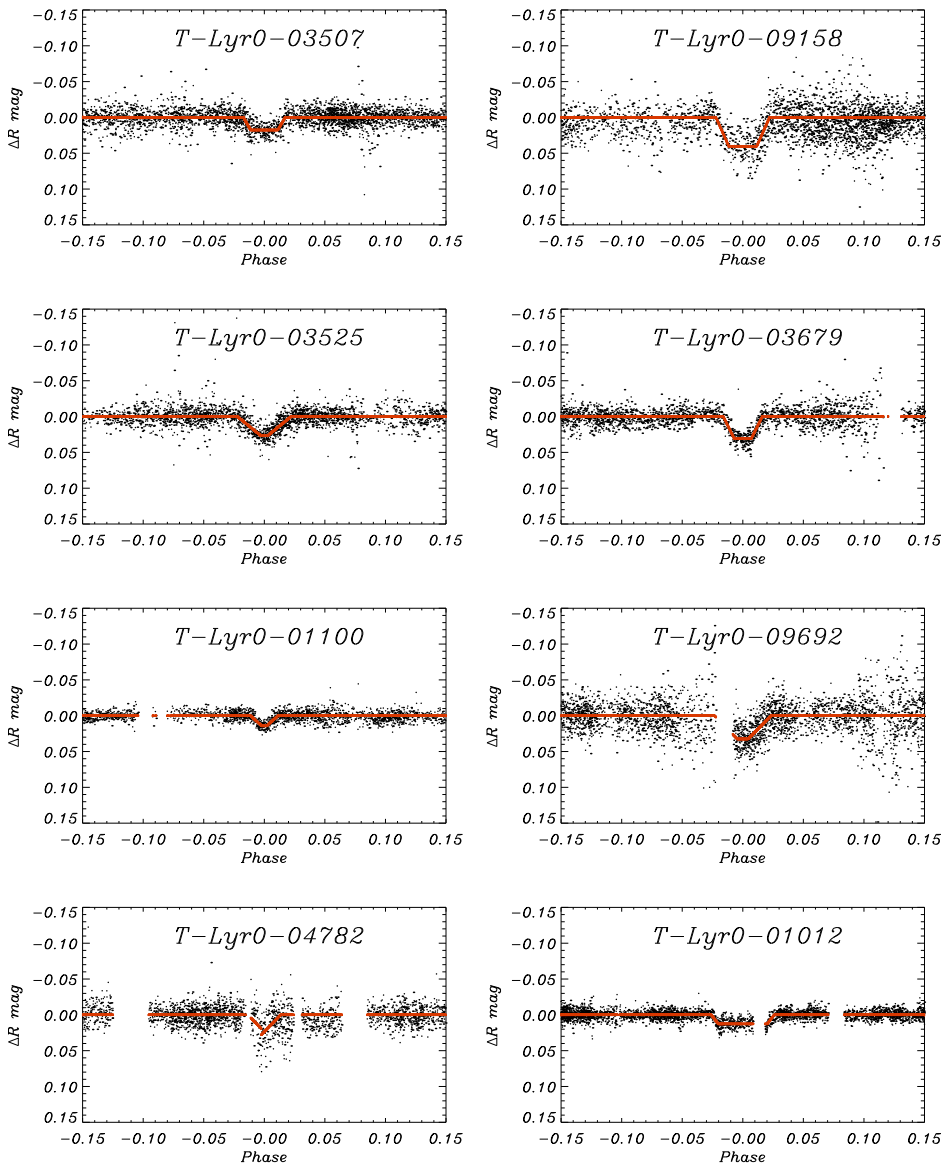

FIGURE 4.8— Transit shape fitting of the candidates in the Lyra field. The free parameters in the least square fit were the phase of the center of the transit, its total duration, depth and ingress (equal to the egress) time. See the text for details.

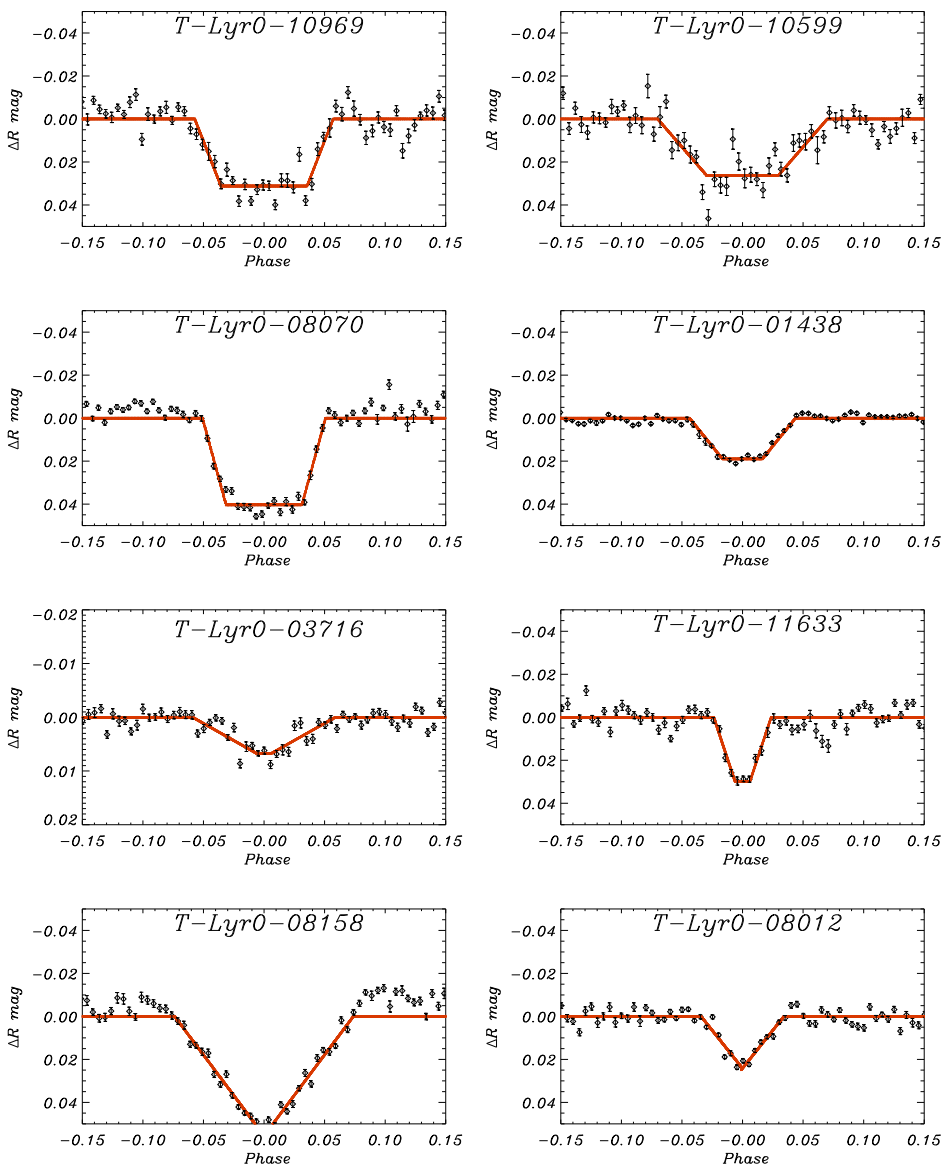

FIGURE 4.9— Same as Figure 4.7, with the data points binned in 0.005 wide bins in phase. The error bars are the *rms* of the N points inside each bin divided by the square root of N.

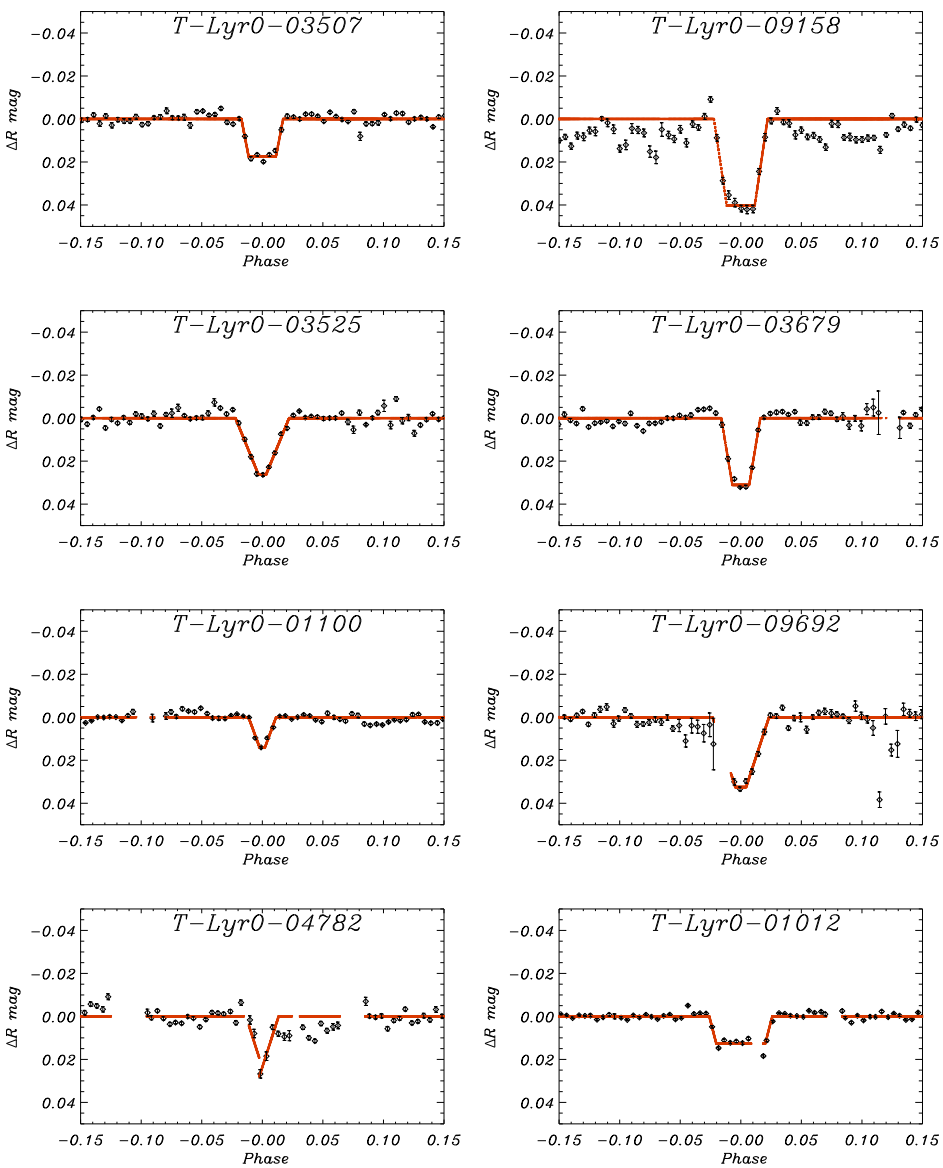

FIGURE 4.10— Same as Figure 4.8, with the data points binned in 0.005 wide bins in phase. The error bars are the *rms* of the N points inside each bin divided by the square root of N.

4.4.2 Out of eclipse modulation

We evaluated the significance of the out of eclipse modulation in each of the candidates, according to Equation 3.2. This was done by a non-linear fit of the phase-folded light curves to the 5 adjustable parameters (<I>,a_{c1},a_{c2},a_{s1},a_{s2}) based on the Levenberg-Marquardt algorithms (Levenberg 1944; Marquardt 1963). The eclipses, with a total duration measured in the previous section, were not taken into account in the fit. Figures 4.11 and 4.12 plot the fits to each of the candidates, superposed on the unbinned data. Figures 4.13 and 4.14 plot only the resulting fitting functions, to highlight the amplitudes of each of the modulations. The values of the significance D_i, defined in Equation 3.3 are printed in Table 4.5. Finally, Figure 4.15 plots the maximum values of these significance. The slash-dotted line in that plot, at a level of D = 3, separates candidates with significant out of eclipse modulation (at a 3σ level from those with non significant modulation). Surprisingly, only 3 out of the 16 candidates were consistent with no modulation. This gives an idea of the utility of this cheap test (i.e., no further observations are needed). The 3 candidates that survived this test were T-Lyr0-03716, T-Lyr0-03507 and T-Lyr0-03525.

Taking this result in addition to that from the previous Section, the only candidate that survived both tests was T-Lyr0-03507, which, as we will see in this and the next Chapter, proved to be the only transiting exoplanet among the 16 candidates. In the next Section, we summarize the spectroscopic and photometric follow-up observations of each candidate, to firm up this conclusion and to try to unveil the true nature of each of the impostors.

4.5 Spectroscopic and photometric follow-up of transit candidates

In this section, we summarize the spectroscopic and photometric follow-up work performed on the 16 candidates obtained in the Lyra field.

4.5.1 T-Lyr0-10969: An eclipsing brown dwarf, M star, or a blended system?

With a flat bottom eclipse lasting 2.45 hours, this short period candidate was compatible with a transit of a planet across a main sequence F-sized star (1.5 $R_\odot$). The 2MASS colors are consistent with an early-mid F star. Three spectra were taken with the CfA Digital Speedometers, revealing a rapidly rotating (80 km/s) F dwarf. The rapid rotation of the star causes the radial velocities to be less precise, but there are weak evidences for variations at the 10 km/s level. Assuming a mass for the primary of 1.5 $M_\odot$ (from Cox 2000),

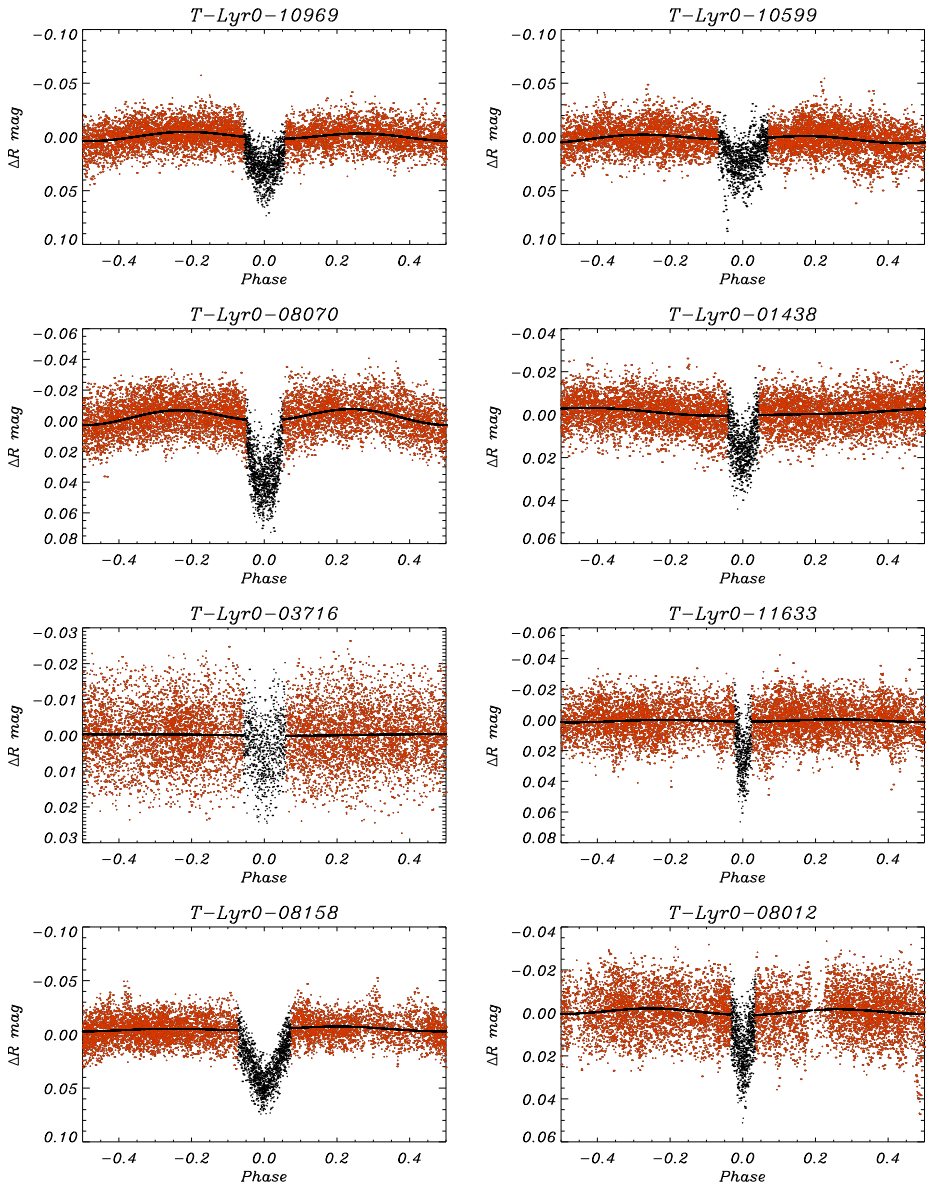

FIGURE 4.11— Folded light curves of the candidates in the Lyra field, together with the best fit to the out-of-eclipse part. The eclipses have not been considered in the fits.

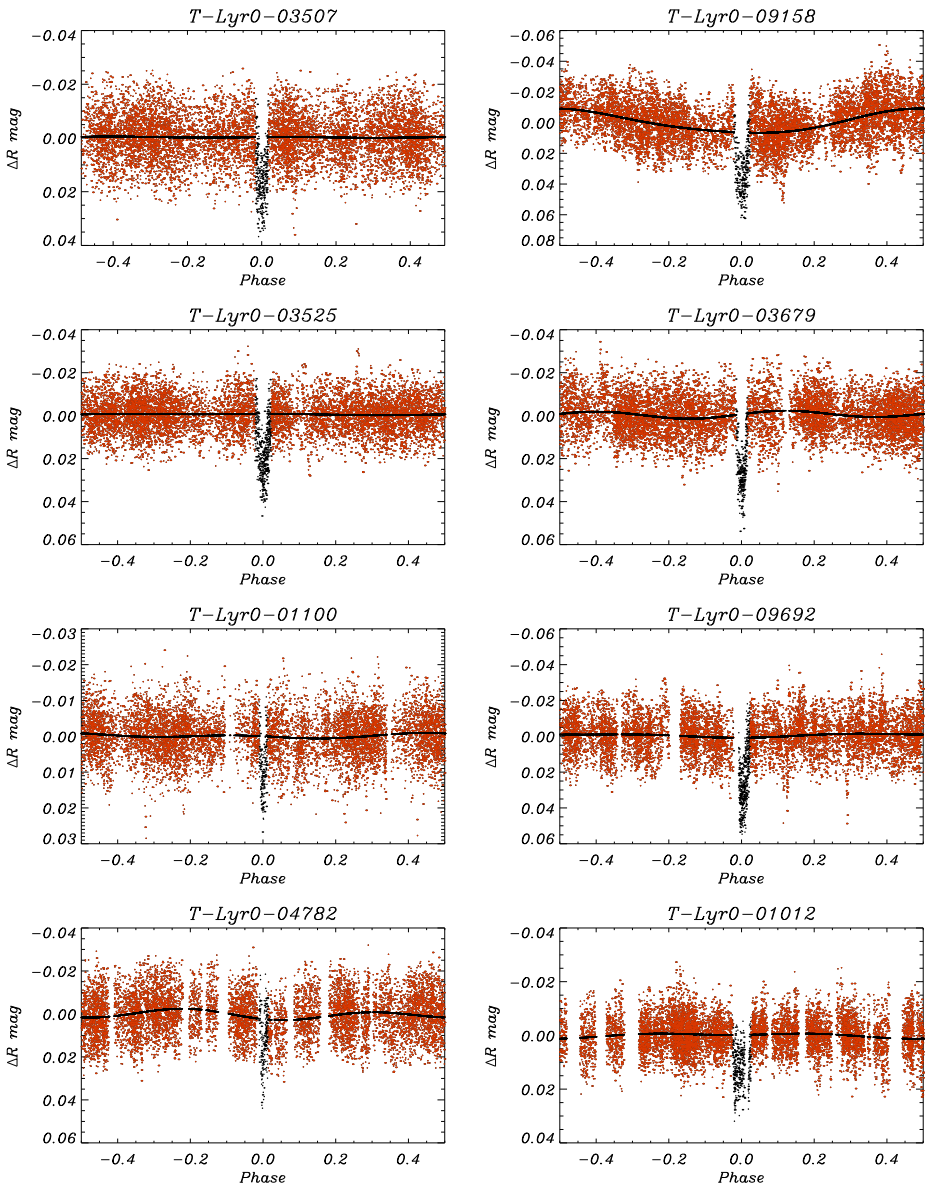

FIGURE 4.12— Same as Figure 4.11

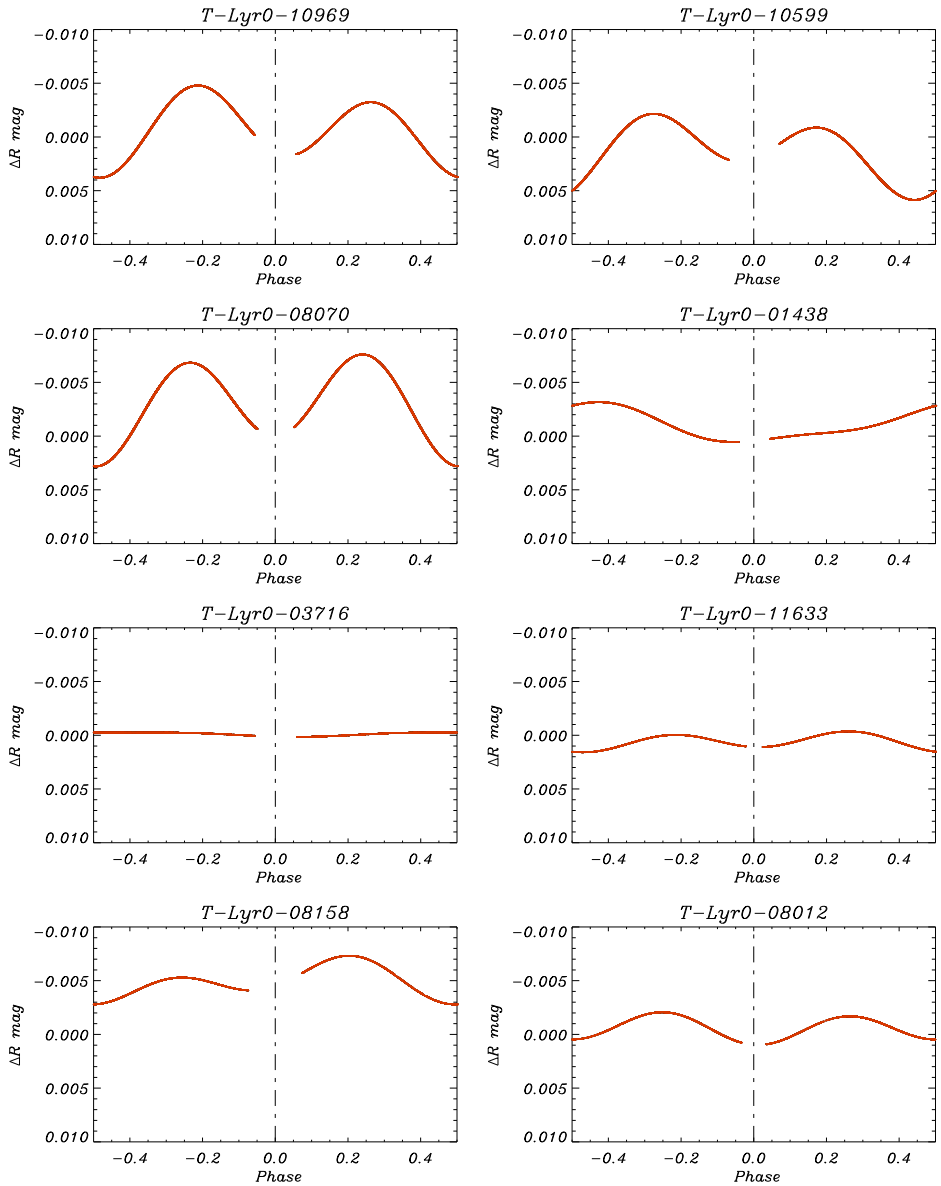

FIGURE 4.13— Ampliation of the best fit solution to the out of eclipse modulation on the candidates, plotted in Figure 4.11.

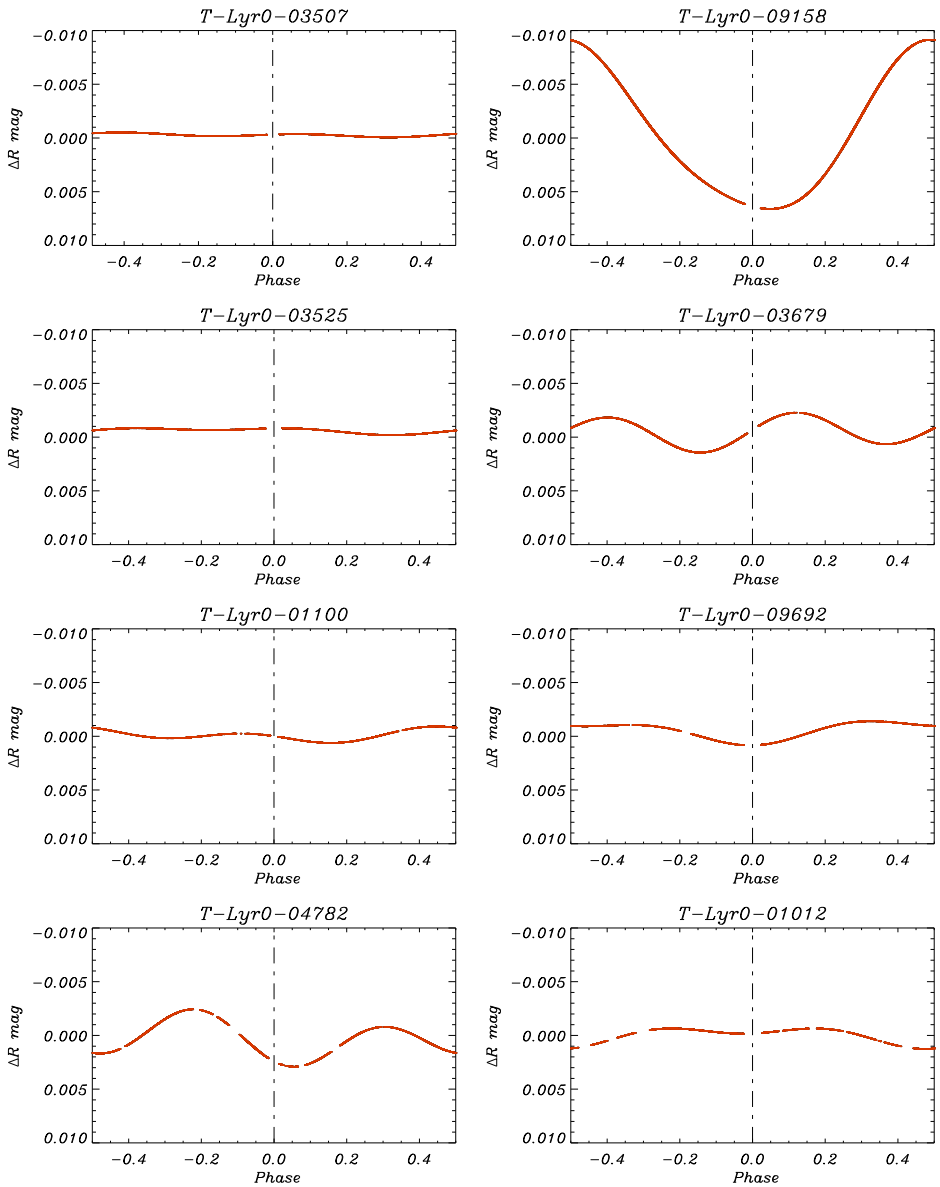

FIGURE 4.14— Same as Figure 4.13, for the candidates plotted in Figure 4.14

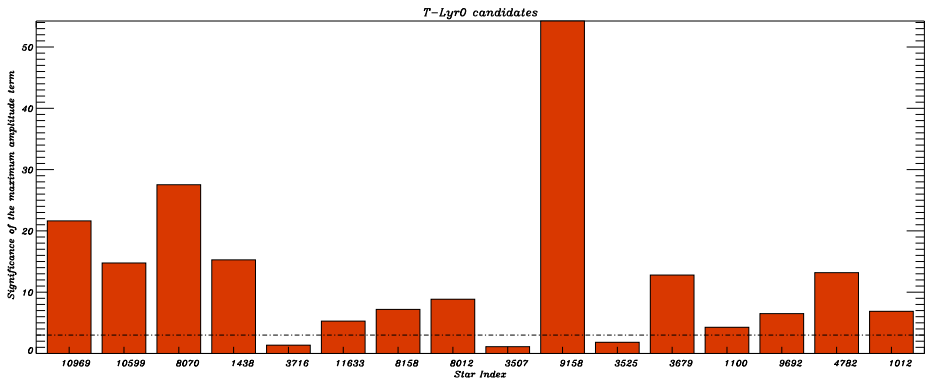

FIGURE 4.15— Values of the significance D_i defined in Equation 3.3 for the out of eclipse modulation in the candidates obtained in the field of Lyra. The 3σ level is overplotted with the slash-dot line. Only 3 of the 16 candidates remain below this level, and thus 13 of the candidates could have been ruled out by this simple method.

TABLE 4.5— Significances of the different terms to the fit described in Equation 3.2.

Candidate	D_{c1}	D_{s1}	D_{c2}	D_{s2}
T-Lyr0-10969	-7.75	4.92	21.63	8.12
T-Lyr0-10599	-9.72	10.47	14.76	-13.58
T-Lyr0-08070	-8.99	-2.93	27.53	0.60
T-Lyr0-01438	15.27	4.20	-1.48	-5.09
T-Lyr0-03716	1.35	0.63	0.34	0.36
T-Lyr0-11633	-1.51	-1.50	5.28	1.52
T-Lyr0-08158	-4.56	-6.03	7.19	-3.61
T-Lyr0-08012	1.70	1.44	8.85	0.56
T-Lyr0-03507	0.33	0.69	-0.67	-1.11
T-Lyr0-09158	54.24	1.65	-6.64	4.53
T-Lyr0-03525	-0.81	1.82	-0.94	-1.23
T-Lyr0-03679	0.61	-3.93	-2.32	-12.80
T-Lyr0-01100	4.27	0.68	-3.79	3.75
T-Lyr0-09692	6.50	-1.28	3.30	0.21
T-Lyr0-04782	2.97	7.00	13.19	6.22
T-Lyr0-01012	-6.88	1.34	5.28	-1.88

this range of velocities would imply a companion of 0.059 $M_\odot$, in the brown dwarf regime.

A companion with the masses in the brown dwarf regime would produce flat-bottomed eclipses when transiting in front of a F-sized star. But the existence of the so-called brown-dwarf-desert argues against this possibility. Better determined velocities could easily move the mass of the secondary to the M-star regime, which constitutes a much more plausible scenario.

In the case of a blended triple system, the rapidly rotating F star would be providing most of the light to the system, and a fainter eclipsing binary (not resolved in 2MASS nor AO images) would make the correlation peaks of the CfA spectra vary, which might be erroneously interpreted as variations in the radial velocities of the F star. The rapid rotation of the star makes it possible that a fainter stellar system remains undetected in the CfA spectra.

With the main star being a fast rotator it is difficult to disentangle which of the two possible explanations for this candidate is the real one. In any case, these transits can not be produced by an exoplanet.

4.5.2 T-Lyr0-10599: A blended triple system

With a period of less than 1 day, this candidate showed flat-bottomed eclipses in its light curve, and in the 2MASS images there were no other stars within 20" and 3 magnitudes in J. The 2MASS colors point to a mid F star. The total duration of the transits (3.1 h) are inconsistent with transits of a planet in a circular orbit around a main sequence star (see Figure 1.6).

The analysis of one CfA spectrum indicated a composite spectrum, with a slowly rotating primary and a rapidly-rotating secondary. The flat-bottomed eclipses together with this evidence for a composite spectrum is a proof for an (at least) triple system. Furthermore, the presence in the spectra of two signals of stars with different rotations could only be explained if the system had not enough time to be tidally locked. With such a short period, the tidal timescale for locking of, for instance, an 1.5 $M_\odot$ F star and a 0.3 $M_\odot$ star, is $\sim$37000 years (from the Equations in Marcy et al. 1997). This reinforces the triple star hypothesis.

A plot of the light curve binned as in the previous case (average of 64 data points per bin) is given in Figure 4.16. If we add the results of the out of eclipse modulation and stellar density measurement from the previous Section, we can conclude that there must be an unresolved eclipsing binary, constituting a blended triple system.

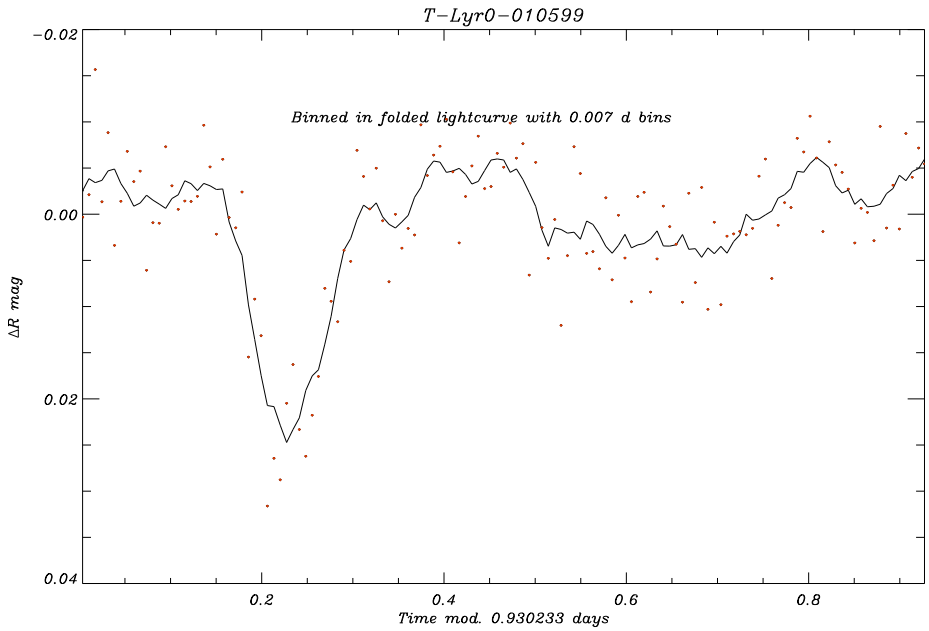

FIGURE 4.16— Light curve of T-Lyr0-10599 folded with the best found period and binned in phase. Each point is an average of typically 60-70 data points. The solid light curve is the 6-points median-filtered light curve. After follow-up observations, this candidate proved to be a blended triple system.

4.5.3 T-Lyr0-08070: A binary system

This candidate has clear flat-bottomed eclipses, that lasted for 2.9 hours, with 1.8 hours in a flat bottom stage. This duration is longer than expected for a solar radius star and the low period of the transits (1.18464 d). If the star is made bigger, so that the duration can match the observations ($\sim$2 $R_\odot$, according to Figure 1.6), then the depth is far too big to be explained with a Jupiter sized object (the implied radius would be 3.7 R_J). Some eccentricity might help to explain the long duration of the eclipses, but then a problem arises on how to explain a non-negligible eccentricity in an object with a period of roughly 1 day. A light curve binned in phase shows an out of eclipse modulation with a semi amplitude of $\sim$5 mmags (Figure 4.17), as expected from the analysis of the out of eclipse modulation carried out in Section 4.4.2.

Four spectra were taken with the CfA Digital Speedometers. These are consistent with a main sequence star of T_{eff} = 6500 K, rotating with a vsini

of 64 km/s. Even with such a high rotational velocity (which broadens the spectral lines, decreasing the precision of the radial velocities measurements), radial velocities changes have a range of ∼20 km/s. This is evidence for a stellar companion to the star. The rotation of the primary, and the period of the secondary, yield a radius of the star of 1.5 $R_\odot$ (assuming tidal synchronization, see Equation 3.12), which is to first order consistent with the determined T_{eff}.

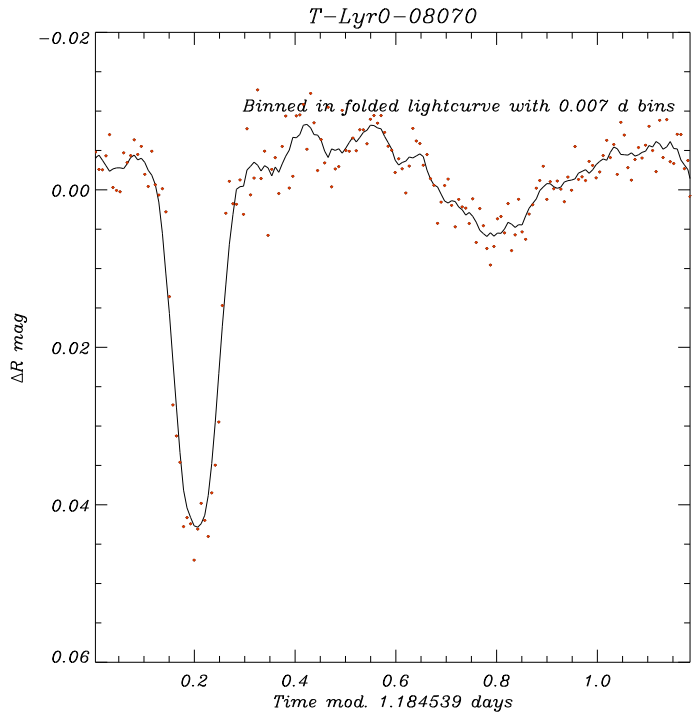

FIGURE 4.17— Light curve of T-Lyr0-08070 folded with the best found period and binned in phase. Each point is an average of typically 50 data points. The solid light curve is the 6-points median-filtered light curve. After follow-up observations, this candidate proved to be a binary system.

4.5.4 T-Lyr0-01438: A binary system

With a period of 1.297404 d, the fit of the transit shape of this candidate revealed 2.7 hour eclipses with a flat bottom duration of 1 hour. If main sequence stars and circular orbits are assumed, then the mass of the central star should be $\gtrsim$1.5 $M_\odot$ in order to reproduce the transit duration (see the Figure 1.6 of

the Introduction).

The spectral type of the star from the 2MASS colors pointed to an early-mid F type star. As expected from the result of the Section 4.4.2, binning in phase the light curve showed out of eclipse modulation with an amplitude of ∼3 mmags (Figure 4.18). This was a clue that the system had stellar components. There are no significant differences between primary and secondary eclipses when the light curve is folded with double the period. Two spectra taken at the CfA showed variations of 50 km/s, and a rotational velocity that implied one solar radius for the star, assuming synchronization with a companion with double the reported period. This confirmed the stellar nature of the system, thus rejecting it as a planetary candidate.

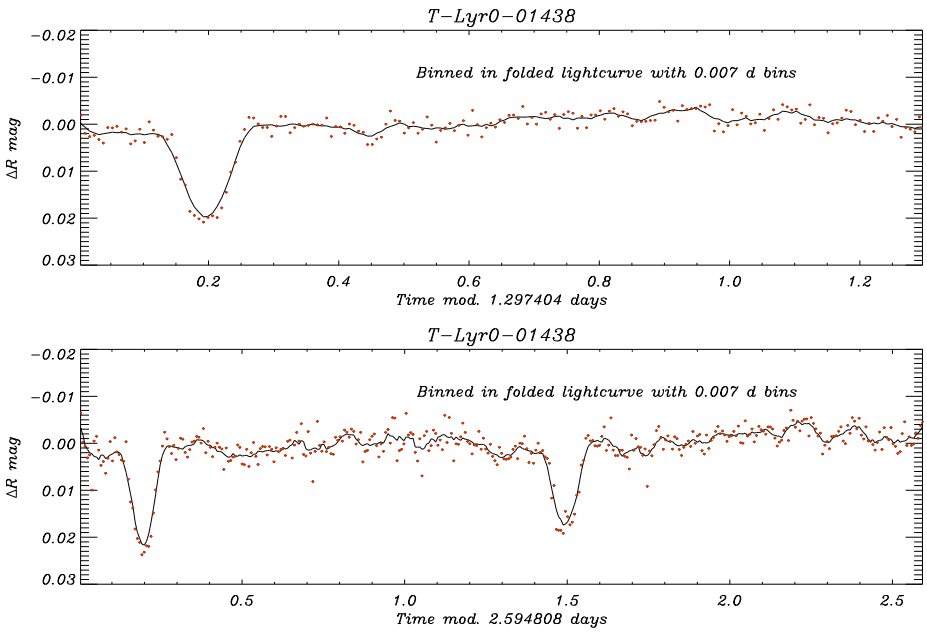

FIGURE 4.18— Light curve of T-Lyr0-01438 folded with the best found period and binned in phase (top). Each point is an average of typically 45 data points. Bottom: the same candidate, but folded with double the reported period. The solid light curve is the 6-points median-filtered light curve. After follow-up observations, this candidate proved to be a binary system, with double the reported period.

4.5.5 T-Lyr0-03716: A blended triple system

Even though the STARE light curve shows a ∼6.8 milli-magnitudes depth transit, the PSST data helped to confirm this as a candidate, with the lowest transit depth of all. The combined and binned data showed a triangular eclipse, as seen in Figure 4.19. The 2MASS colors are compatible with a K star. But, the spectra taken at CfA favor a K giant, and there is no velocity variation at a level of 0.14 km/s. The period of the transit and typical radii for K giant stars (a KIII star has a radius of 15 $R_{\odot}$, Cox 2000) would imply that the companion would be in orbit inside the atmosphere of the star. However, this problem can be solved if we explain the observations with a triple system, where one component is the K giant, and there is a faint main-sequence eclipsing binary in the glare of the giant.

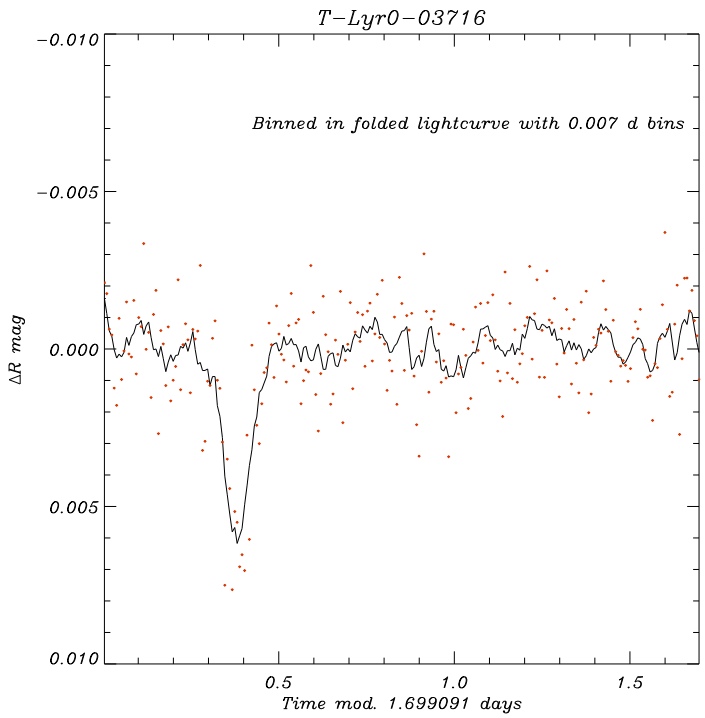

FIGURE 4.19— Light curve of T-Lyr0-03716 folded with the best found period and binned in phase. Each point is an average of typically 50 data points. The solid light curve is the 6-points median-filtered light curve. After follow-up observations, this candidate proved to be a blended triple system.

4.5.6 T-Lyr0-11633: A binary system

The light curve of this candidate showed eclipses lasting for 2 h, and the fit to the transit shape is consistent with a flat transit part of half an hour. Binning the light curve folded in phase with the reported period, and twice this value, showed some tentative differences between primary and secondary eclipses (Figure 4.20). However, these were not conclusive, mainly due to the faintness of this candidate in the STARE images, what causes the dispersion of the data to be 0.024 mags in the raw (unbinned) data.

The 2MASS colors indicate a mid F or an early G type star. Three CfA exposures showed a variation in radial velocities with a total range of almost 60 km/s. This is not consistent with a planetary mass companion, so this object was not further observed.

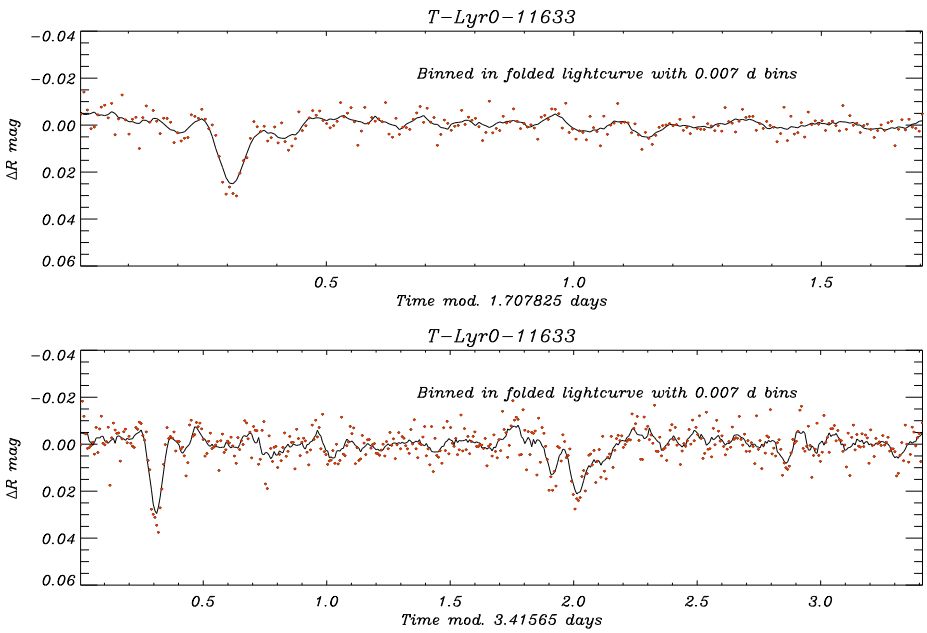

FIGURE 4.20— Folded light curve of T-Lyr-11633, with the reported period (top) and twice this value (bottom). The CfA radial velocities showed this was a stellar binary system.

4.5.7 T-Lyr0-08158: A blended stellar system

This star exhibits triangular-shaped eclipses. A binning in phase with the photometric period (1.873396 d) and twice this value does not show detectable differences among a primary and a secondary eclipse (Figure 4.21). There is a star 2.4 magnitudes fainter in J at 7″, easily resolved in the 2MASS images. The duration of the eclipses is ∼7 hours, inconsistent with a transit of a planetary companion with this period, in a circular orbit. 2MASS colors point to a mid-K star, while the CfA spectra (not showing detectable radial velocity variations) favor a G dwarf. Both the duration and the shape of the eclipses can not be explained by a transiting planet, and the most plausible scenario is the star at 7″ being an eclipsing binary with almost equal components. In this case, the undiluted eclipse depth would be of ∼48.5%, which favors the hypothesis of undistinguishable primary and secondary eclipses, both stars being of similar size and luminosity. The J–K colors of this star are compatible with a mid-G spectral type.

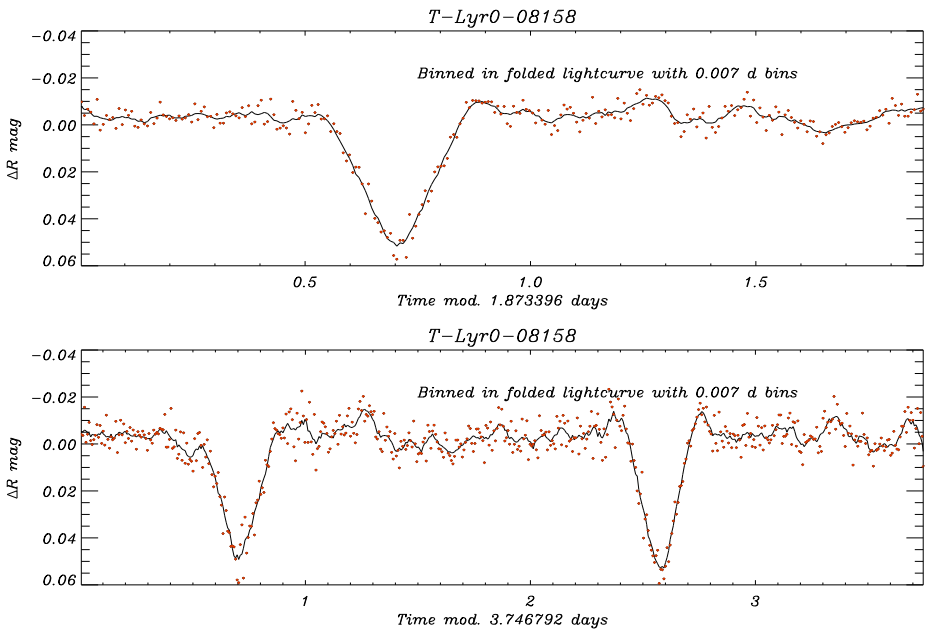

FIGURE 4.21— Folded light curve of the candidate T-Lyr-08158 with the best-found period (top), and twice this value (bottom). There are no significant differences among the primary and secondary eclipse in the bottom plot. After follow-up observations, this candidate proved to be a blended stellar system.

4.5.8 T-Lyr0-08012: A blended stellar system

As we saw in Section 4.4.2, this star showed significant out of eclipse modulation, and the fit to the transit shape revealed a triangular eclipse, with no flat bottom (see Table 4.2). The duration of a grazing planetary transit, for a 1 $R_{\odot}$ star, would be of ∼1.6 h, which is much smaller than the fitted total transit duration of 4.5 hours. Four spectra of this candidate were taken at the CfA, showing a slowly rotating star with a T_{eff} of 6000 K, consistent with the J–K determined spectral type (late F or early G). The measured radial velocities are consistent with no variation, down to residuals of 0.6 km/s.

There is a companion 2 mags fainter at a distance of 21″. The out of eclipse modulation, the transit shape fitting and the absence of radial velocity variations suggest that this companion is an eclipsing binary, whose light is diluted by the candidate, thus constituting an obvious blended case. As the angular separation of the components is relatively high, the more plausible scenario is a fortuitous alignment of the two resolved stars, with no gravitational binding. The undiluted eclipse depth of the binary would be 17.2% in J.

4.5.9 T-Lyr0-03507: A transiting planet

This candidate will be discussed in further detail in the next Chapter. After the confirmation that this star had a Hot Jupiter producing transits, this star was renamed as TrES-1 parent star. The period that returned the maximum value of the SDE was half the real period. This circumstance is due to the period being close to an integral number of days, which causes the phases at a distance of 0.5 from the transits to be poorly sampled (see Figure 4.5). The PSST data served to identify the real period, as no transits were observed in the phases that were poorly sampled in the STARE data.

4.5.10 T-Lyr0-09158: A binary system

This star showed flat-bottomed eclipses in the binned light curves, and there was evidence for out of eclipse modulation, greater than 10 mmags amplitude (Figure 4.14). Both J–H and H–K are consistent with a G type star. The CfA spectra are also consistent with a G type star, but the rotation is bigger than that expected for a dwarf star synchronized with a stellar companion. Three spectra spanning 6 days showed velocity variations of more than 10 km/s, also rejecting this star as a planetary candidate. A plausible model for this system is a slightly evolved G star with a stellar companion. The evolved stage of the star would result in an increased radius, and thus the eclipses of the secondary component could have depths comparable to those produced by a transiting planet across a dwarf star, and also a flat part of the transit. The results of the

out of eclipse modulation test performed in Section 4.4.2 showed a significant contribution of the $\cos p_k$ term into the fit. A more realistic situation would be that the real period is twice the reported period, showing an eclipsing binary with indistinguishable primary and secondary eclipses, and with the out of eclipse modulation being a consequence of the ellipsoidal variability instead of the more improbable reflection effect. In Figure 4.22 we show plots of the binned data, for both cases.

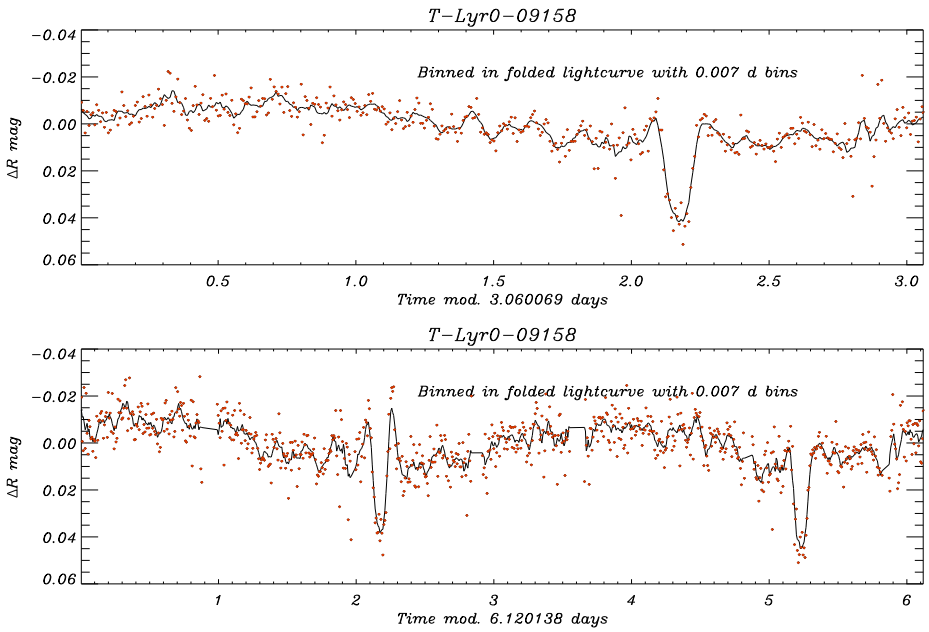

FIGURE 4.22— Folded light curve of the candidate T-Lyr-09158 with the best-found period (top), and twice this value (bottom). There are no significant differences among the primary and secondary eclipse in the bottom plot. After follow-up observations, this candidate proved to be a binary system.

4.5.11 T-Lyr0-03525: A grazing binary

Even though the raw light curve does not show evident flat-bottomed transits, the fit to the transit shape is compatible with a short flat part, of ∼30 min. If there is a transiting planet at high enough latitudes, it could produce transits without a flat bottomed part (if the orbital inclination of the system is between the values stated in Equation 3.1.1). The depth could be compatible with a

planetary transit, and the 2MASS colors are consistent with a F-G dwarf star. There are two stars, at 22″ and 42″ respectively, that are less than 3 mags fainter in J. In the case that these are eclipsing, the depths would have to be of less than 12% in order to reproduce the observed depths (equal to 12% for the star 2.9 mags fainter located at 22″). However, two exposures taken at the CfA showed a double lined binary with almost equal components. This rejects the hypothesis that the relatively close companions are eclipsing. The system is a grazing binary.

4.5.12 T-Lyr0-03679: A blend

The light curve of this candidate shows a 0.031 mags flat bottomed eclipse lasting for ∼2.9 hours, consistent with transits of an object with a radius of 1.7 R_J across a 1 $R_\odot$ star. If the star were smaller, of a size of 0.6 $R_\odot$, then a planet with a radius of 1 R_J could explain the observed depth. But, in this case, the total duration of the transit would be bigger than the maximum duration for circular orbits (see the Figure 1.6 of the Introduction). Some eccentricity might explain the longer duration of the transits, if these are happening closer to the apastron than to the periastron.

The 2MASS images (Figure 4.23) showed two close stars, at an apparent distance of 7.9″, and with a difference in J magnitudes of 1.8. As both stars fall inside the PSF of the STARE images, we can not know which of the two stars is being eclipsed. We will refer as component A to the star GSC 02665-00795 (the brightest one) and component B to the star 2MASS 19203383+3637402 (the faintest). If the component A is having the eclipses, the real depth would be diluted, and the corrected depth, taking into account the flux from component B, would be 3.35% instead of 2.81%[2]. This way, a planetary object might be the source of the transits, even if they are diluted (a 1.3 R_J planet would match the observations if we assume a radius for the A component of 0.75 $R_\odot$, based on its 0.614 J–K color.). But, if the eclipsing companion is around component B, the corrected depth would be of 17.6%[3], and thus it could not be explained by transits of a planetary object (the implied radius would be of 3 R_J).

In order to find out which of the component was having the eclipses, we observed the system at the 82-cm IAC80 telescope, on the night of June 28th 2004. Due to the nature of this case, we observed completely in focus, to be able to perform aperture photometry on each of the two stars, as well as in several reference stars. The final light curves, obtained in V an I filters, are plotted in figures 4.24 and 4.25. In those figures, we have also plotted the signal we

[2] $k = 1 - \frac{(F_A+F_B)10^{-0.4*0.031}-F_B}{F_A}$, where $F_A = 10^{-0.4*m_A}$ and similarly with F_B

[3] $k = 1 - \frac{(F_A+F_B)10^{-0.4*0.031}-F_A}{F_B}$

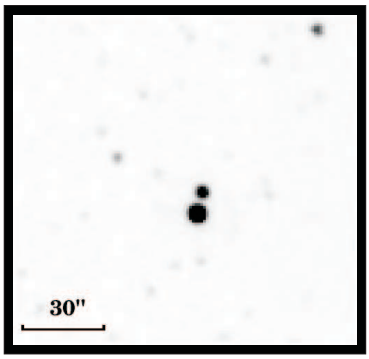

FIGURE 4.23— 2MASS image of the candidate T-Lyr0-03679, revealing the presence of two close stars, at a separation of 7.9″.

would have obtained if the system had not been resolved, by adding the fluxes of both stars. A flat bottomed eclipse is clearly seen in the V filter. The V–I color of the blended system would have shown a slight signal in the transit phase (Figure 4.26), which indicates that the blended system appears redder while in transit. This is the opposite effect as the limb-darkening wavelength dependence; in this case, the limb-darkening effect is more noticeable at shorter wavelengths (e.g., Claret 2000). The transit shape, in the case of a planet, would thus be flatter at longer wavelengths. This would leave a colored signal that would make the star appear slightly redder in the ingress and egress phases, and bluer in the central parts of it (see, for example, the colored light curves of HD 209458b by Charbonneau et al. 2003). The observed contrary effect means that *i)* the companion can not be a transiting planet, and *ii)* the "third" star (i.e., the one that is providing most of the flux to the system, component A in our case) is redder than the brightest star in the eclipsing system (component B). This is confirmed with the 2MASS colors ($(\mathrm{J–K})_A = 0.614$, $(\mathrm{J–K})_B = 0.510$).

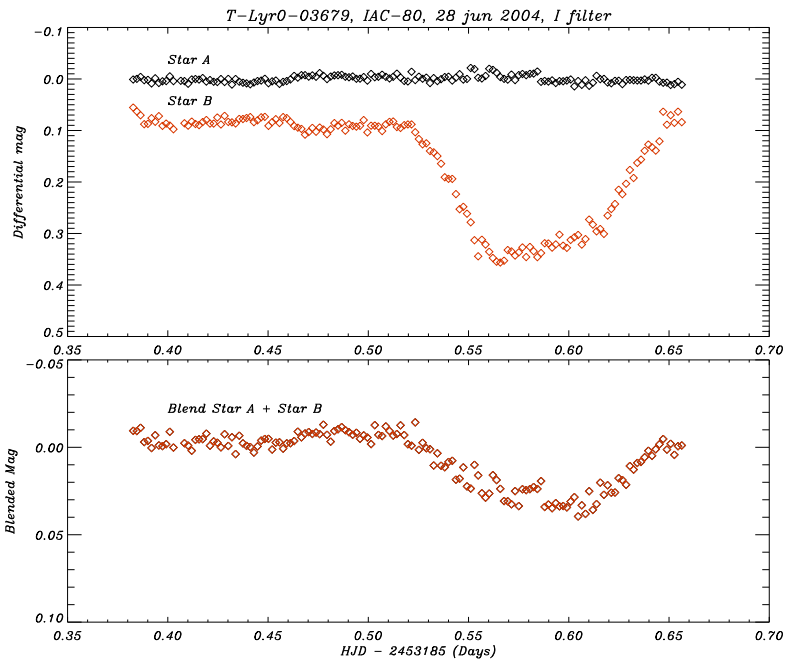

FIGURE 4.24— I-filter differential light curves obtained at the IAC80 telescope. Top: the two individual light curves of each of the components, revealing a flat-bottomed eclipse in the faintest star. Bottom: the observed light curve if we add the fluxes of the two components (the same effect as if we had not resolved the system).

4.5.13 T-Lyr0-01100: A blend

The light curve of this object seems to show a flat bottomed eclipse. The 2MASS images reveal two close (8.2″) stars with similar brightness. Assuming both stars are of identical brightness, the undiluted depth of the transits would then be 0.028 mags. The 2MASS colors of these stars point to two mid-F stars. Thus, the radius of an object capable of producing 0.014 mags depth transits in the blended system would be of 2 R_J (assuming a radius for the F star of 1.3 $R_\odot$).

The observations obtained at the WHT with NAOMI showed that one of these two stars was indeed a double star (see later, Figure 4.29). All the three stars have a similar brightness in K filter. The distance of this third star to its closest companion is ∼0.8″. With three stars of similar brightness blended, the radius of an object that can cause the observed transit depths is now ∼2.5 R_J, if we assume that it is orbiting around one of the two F stars. There are no big

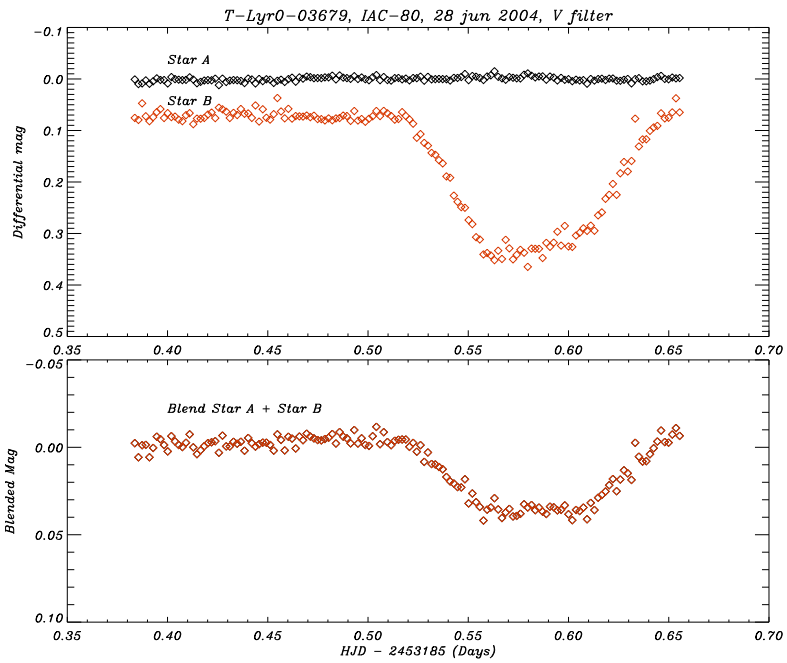

FIGURE 4.25— Same as Figure 4.24, for the V filter.

inconsistences among the spectral types of the two stars resolved in the 2MASS images, when estimated from the J–H and from the H–K colors (see Table 4.1). This indicates that the newly found star might have a spectral type similar to the other two, and thus also a similar radius.

4.5.14 T-Lyr0-09692: A diluted triple system?

The STARE light curve of this candidate showed evidence for three egresses of a transit with a period of 6.199628 d. J–H colors suggest an F6 spectral type, while the H–K point to a K4 star. This discrepancy might be resolved with the assumption of a blended system. There are clues for out of eclipse modulation, as we saw in Section 4.4.2. The CfA spectra showed radial velocity variations of more than 30 km/s, and rotational velocities not compatible with tidal synchronization. This circumstance can arise if the stellar system is composed of an eclipsing binary diluted by a third star (the measurement of the rotational velocity being affected by the contribution of a secondary unresolved moving correlation peak).

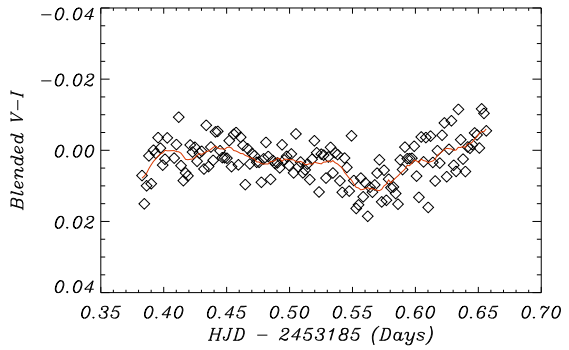

FIGURE 4.26— V–I color signature of the eclipse of the system T-Lyr0-03679, as would have resulted if the system had not been resolved. The color pattern of the eclipse is the opposite as expected for a transiting planet (see text).

4.5.15 T-Lyr0-01012: A binary system

This candidate showed a flat-bottomed eclipse lasting for at least 12 hours. Its period, of more than 10 days, was specially interesting, as a transiting planet found with such a long (in terms of transit searches) period would provide some clues on the dependence of the inflation of the planet due to the central star insolation, and thus to solve the paradox of the radius of HD 209458b (see the Introduction, 1.4).

STARE recorded one whole night in transit, one ingress and one egress. PSST recorded also one ingress, one egress and a whole night in transit, but all were different events (after that whole night in transit in the STARE data, the egress of the transit was recorded in the PSST data set). Combining both data sets gave a clearer light curve, but, when folded with double the period, there is still place for a secondary eclipse that would have not been observed. As seen in Figure 4.27, the ingress recorded from the PSST site seems to go further down than the bottom flat part of the primary eclipse. The total duration of the transit is also incompatible with a transiting planet across a F star, if its orbit is circular (∼5.2 h, see the Figure 1.6). Adding some eccentricity to the system[4] could solve the problem of the transit duration, as the orbital velocity at apastron varies from the circular orbital speed by a factor of $\sqrt{(1-e)/(1+e)}$.

[4]With periods in this range, the eccentricities can be significant, as is the case of HD 217107b with a period of 7.11 days and eccentricity of 0.14 (Fischer et al. 1998), or HD 108147b with a period of 10.9 days and eccentricity of 0.49 (Pepe et al. 2002b)

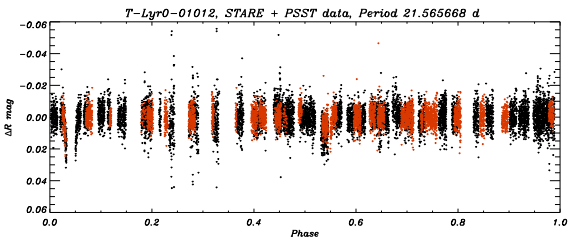

FIGURE 4.27— Phase folded light curve of the combined STARE + PSST data, with double the period reported in Table 4.2. There is still the possibility for deeper primary eclipses that would have not been recorded in any of the data sets (at a phase of ∼0.04). After follow-up observations, this candidate proved to be a binary system.

In this case, though, eccentricities bigger than 0.8 are needed to explain a 12 hours-long transit, and the orientation of the orbit should be such as to produce the transits near the apastron.

Three CfA spectra spanned in 6 days showed velocity variations of more than 50 km/s, thus rejecting it as a transit candidate. The J–K colors are significantly bluer than the effective temperature determined from the spectra, thus suggesting a hot blue companion.

4.5.16 T-Lyr0-04782: An unsolved case

There is only one whole transit event of this candidate, showing a ∼0.028 mags eclipse with a duration of ∼6 h. Folding the light curve with a period of 9.22 d gives a possible solution, and a SDE value that allowed its identification. But, as only one transit event was recorded in the STARE data, and none were detected in the PSST data set, this period should be considered with skepticism, and as a minimum value of the period, under the assumption that this event is real and not an artifact of uncorrected atmospheric extinction or other instrumental effects. Two CfA exposures taken 4 days apart showed no velocity differences, and a slowly rotating star.

4.6 Adaptative Optics observations of the candidates

Some of the candidates in the Lyra field were observed at the 4.2 m WHT, with the NAOMI AO system (Myers et al. 2003), and recorded in the infrared INGRID detector (Packham et al. 2003), on the nights of 4 and 5 July 2004. The brightness of the candidates identified by any of the TrES telescopes makes it possible that the stars themselves act as the reference stars necessary to close

the AO loop. The data were taken mostly in J filter, moving to H and K when the target showed interesting features, or some doubts were raised on the single nature of the candidates (i.e., no close companions). A dithering pattern of 5 points was used in each candidate to avoid bad pixels and to perform better measurements of the sky level. The resulting snapshots of the candidates that were observed at this stage are plotted in Figures 4.28 and 4.29. As a consequence of these observations, the candidate T-Lyr0-01100 was found to consist on three unresolved stars with similar brightness, two of them lying at an angular distance of only $0.8''$.

4.7 A challenging false positive detected by TrES: the case of GSC 01944-02289[5]

As an example of a particularly difficult false positive identified by the TrES network, we describe in this section the case of GSC 01944-02289, found in a field in the constellation Cancri. Both multicolor photometry and radial velocity observations (see Figure 4.30) suggested that the system was formed by a substellar object in orbit around an F-type star. The companion mass was estimated (from the CfA radial velocities) as $\sim$32 M_J, which would have placed the object in the brown dwarf regime, and thus would constitute the first observations of transits of this type. Merely the detection of such an object in a tight orbit (with a period of 3.35 days) would have been of great interest, because of its location in the so-called "brown-dwarf desert" (see the Introduction). But the fact that it transited its host star would allow measurements of the sizes and densities of these objects, something that has never been done. Thus, special care was needed in the follow-up of this system.

A careful analysis of the spectral line shapes revealed a non-symmetrical behavior that could be explained assuming the presence of a fainter star whose movement would affect only the upper parts of the stellar lines. A model consisting of three blended stars, in which two are eclipsing and the other is providing light to the system (thus diluting the eclipses), served to derive the properties of the three components. With these properties, it was possible to identify a second set of spectral lines, corresponding to the primary star in the eclipsing system (Figure 4.31). Under this consideration, the photometric and spectroscopic observations can be explained by a hierarchical triple, in which a slightly evolved F5 primary (with $v\sin i\sim$34 km/s, providing $\sim$89% of the total flux) dilutes the eclipses of an M3V star passing in front of a G0V star.

Until today, this TrES candidate has proven the most difficult case of false positive to identify, a cautionary to be remembered when identifying a transiting

[5] A complete description of this work is found in Mandushev et al. (2005)

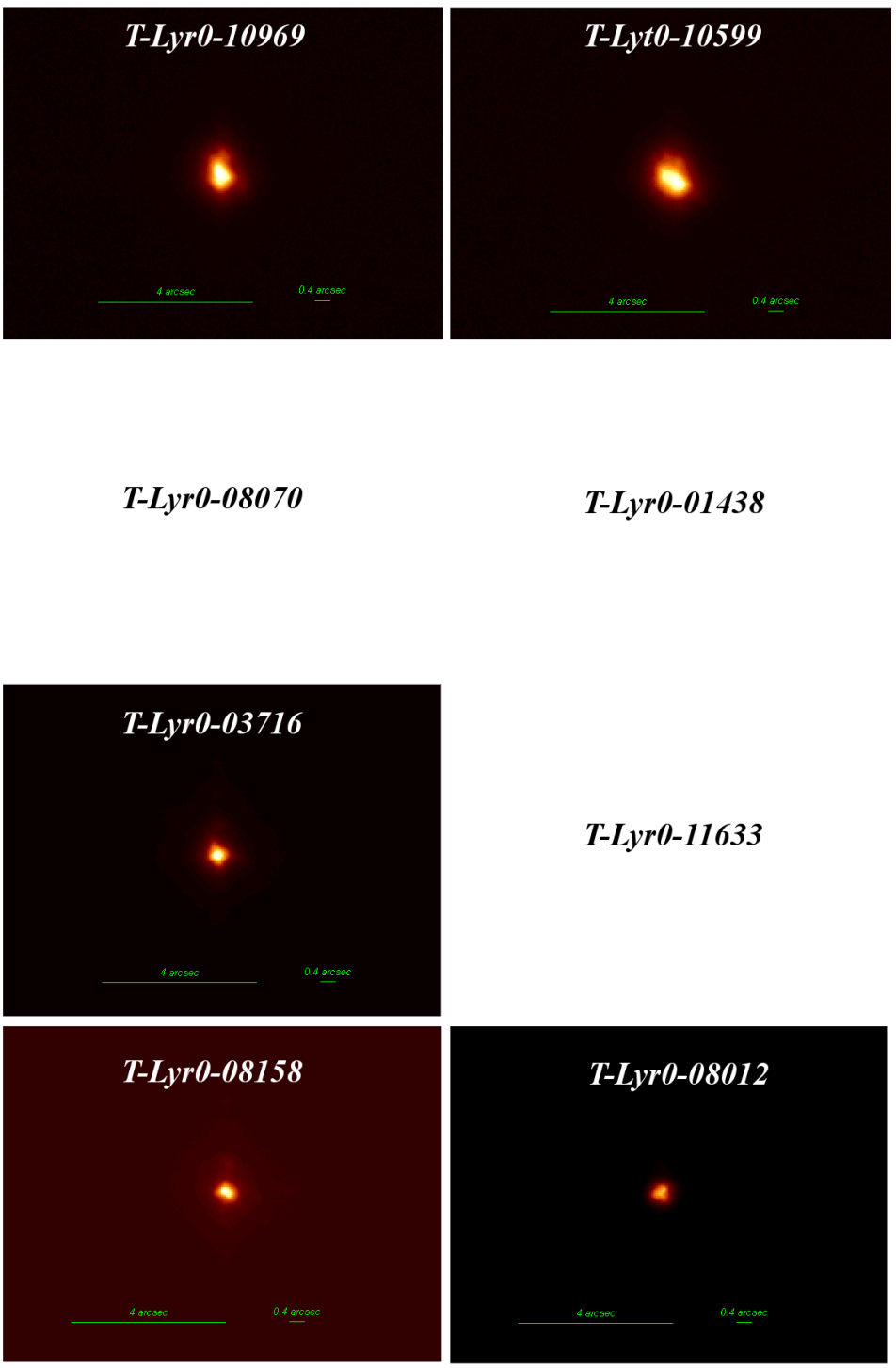

FIGURE 4.28— AO of the candidates, observed with the NAOMI/INGRID system at the 4.2 m WHT telescope. Each image samples roughly a single STARE's pixel (11″).

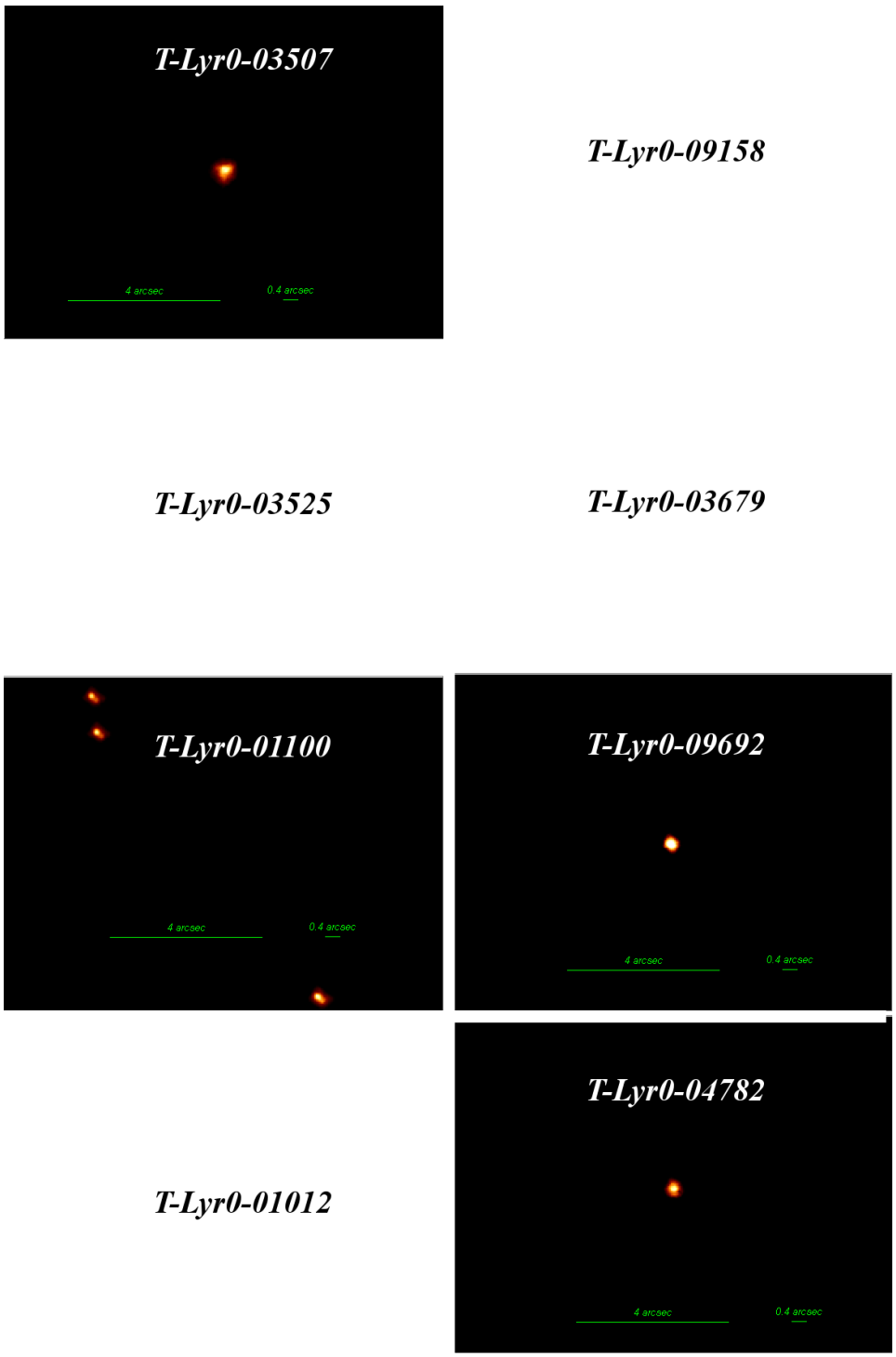

FIGURE 4.29— AO of the candidates, observed with the NAOMI/INGRID system at the 4.2 m WHT telescope. Each image samples roughly a single STARE's pixel (11″). Note the triple system T-Lyr0-01100.

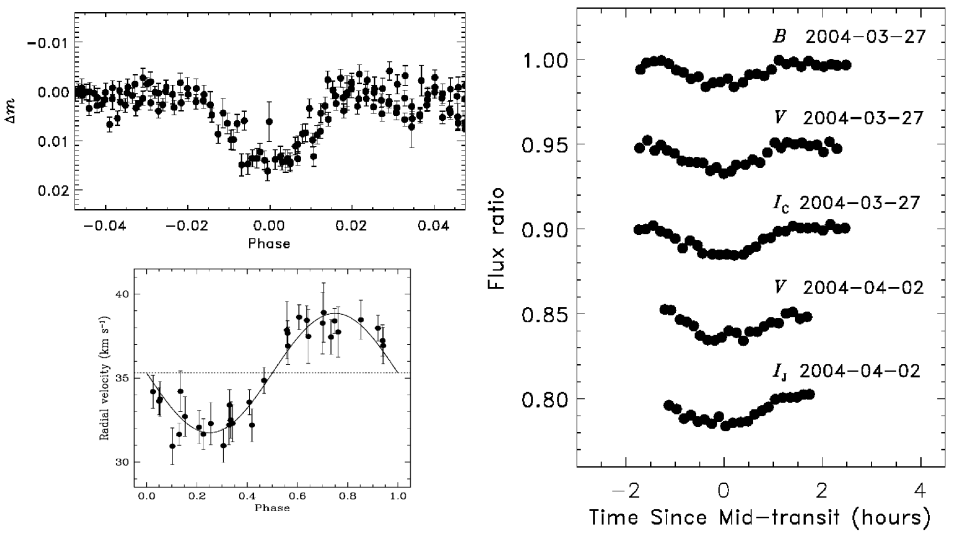

FIGURE 4.30— Top left: The PSST binned phased light curve of the star GSC 01944-02289 (with a period of 3.35 d), showing a 1.4% eclipse with a total duration of 2.7 h. Right: Multicolor photometry of transits of the same star. Bottom left: The CfA radial velocity curve, with an amplitude consistent with a brown dwarf companion.

planet (or brown dwarf) candidate around an F star.

4.8 Results on other stellar fields: a summary of the follow-up on TrES transiting planet candidates.

After almost two years of coordinated observations of STARE as a member of the TrES network, a total of 14 fields have been observed (see Figure 4.32), and the data reduction and analysis of most of them are continuously under way. Typically between 5 and 20 transiting planet candidates in each field are identified, depending on the number of stars present in the field. In this Chapter, we have provided a detailed analysis of one of these fields pointed towards the constellation Lyra, paying special attention to the details of the follow up observations and analysis of the candidates. We have shown that a careful analysis of the light curves can help to discard most of the candidates without the need for extra observations, a philosophy that will be adopted by the members of the TrES collaboration from now on, to provide priorities in the spectroscopic follow-up of each candidate.

To date, a total of 46 false positives in 9 reduced fields have been identified

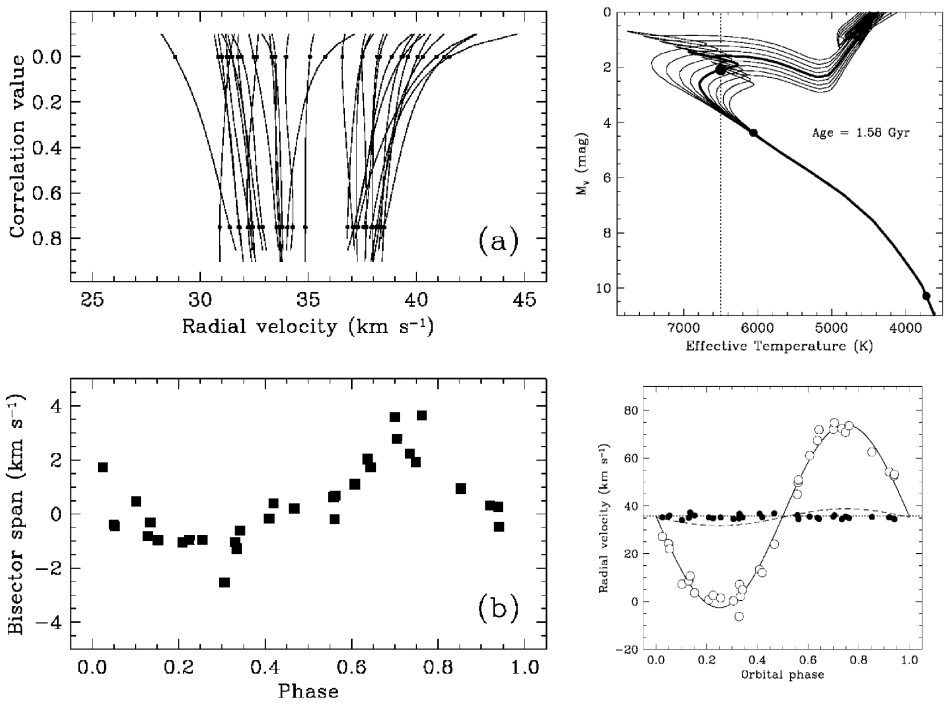

FIGURE 4.31— Top left: The line bisectors of the CfA spectra, showing a wider velocity range in the top of the lines than in the bottom. Bottom left: The bisector span, defined as the velocity difference between the top and the bottom of the spectral lines. Top right: The location in the H-R diagram of the three stars that best explain the data. Bottom right: The extracted radial velocity curve of one of the stars in the eclipsing system (the G0V star, open circles) and the star providing most of the light to the system (the evolved F5 star, filled circles).

in the TrES light curves, 17 of them were discussed in this Chapter, and the follow up work on the rest of them revealed:

- 15 Binary systems
- 7 Blended systems (three or more stars)
- 7 Unsolved cases: binary or triple systems, but, in any case, false positives. If the star is too hot, it is not possible to determine the radial velocities with accuracy. In this case, its radius will also be large, and thus the depth of the transits can not be reproduced by a Jupiter-sized object.

Another 42 candidates are scheduled for follow-up observations, or have survived the low S/N radial velocity measurements. With these number of candidates and detected false positives, it is still too early to provide detailed statistics on the detection rates of false positives, in order to compare them with the expected detection rates stated by Brown (2003). This argument is reinforced by the fact that these expected detection rates are approximate by a factor of a few, due to the number of (necessary) approximations performed in that work. A more detailed analysis of both the expected detection rates (for instance, extending it to other galactic latitudes) and the observed detection rates (considering non trivial factors as the dependance of the detectability of a transit on its duration, depth, crowding, photometric precision, etc.) is out of the scope of this thesis, but might be the objective of future works.

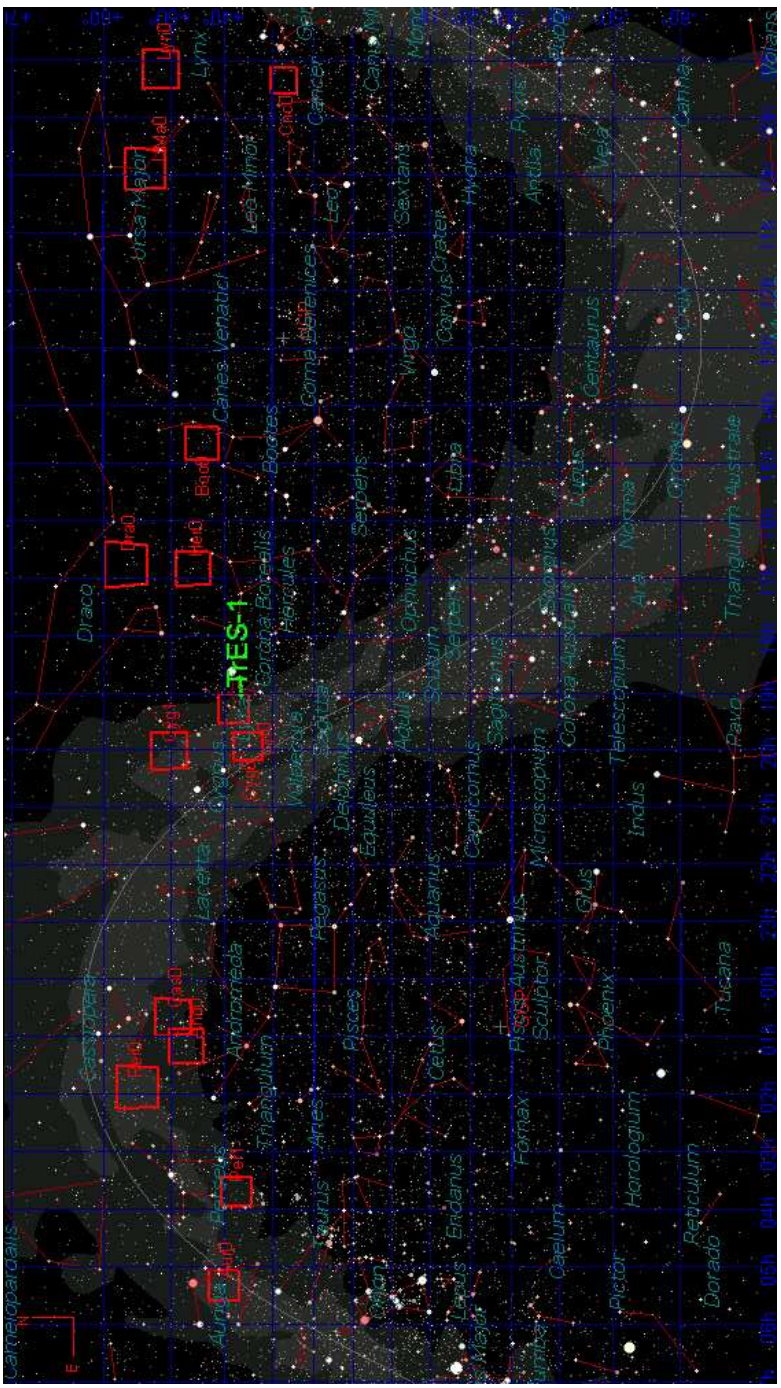

FIGURE 4.32— Location of the TrES network observed fields, in a Mercator projection.

4.9 Conclusions

We have obtained a total of 16 transiting planet candidates, from the observation of a field in the constellation Lyra. Careful analysis of the light curves, spectra taken for the determination of radial velocities, multicolor photometry at 1-m class telescopes, and AO imagery at the WHT have allowed us to classify these candidates as:

- 6 Binary systems: Two stars with ratios of the radii similar to the ratio of a main sequence star-giant planet, or eclipsing stars with grazing eclipses.
- 7 Blended systems: At least three stars, with two of them forming an eclipsing system, and the third star diluting the depths of the eclipses. This third star can be a part of the system, or in the line of sight.
- 2 Doubtful candidates:
  - One seems to be either a triple system, an F+brown dwarf binary or an F+M star binary. The rapid rotation of the brightest star makes it difficult to distinguish among these options.
  - Another has only one observed transit event, and thus undetermined ephemerides. There is also the possibility that the transit event is an instrumental effect.
- A planetary transit candidate, the only one that survived a detailed analysis of the light curve and all the follow up observations aimed to detect false positives. A detailed follow up on this object is the subject of the following Chapter.